

Modeling of the effect of non-spherical particles of various
sizes using Direct Laser Deposition (DLD)



Author

MURSALEEN SHAHID

Regn Number

00000204954

Supervisor

DR.KHALID MAHMOOD

DEPARTMENT OF MECHANICAL ENGINEERING
COLLEGE OF ELECTRICAL AND MECHANICAL ENGINEERING
NATIONAL UNIVERSITY OF SCIENCE AND TECHNOLOGY
RAWALPINDI
SEPTEMBER , 2020

Modeling of the effect of non-spherical particles of various sizes
using Direct Laser Deposition (DLD)

Author

MURSALEEN SHAHID

Regn Number

00000204954

A thesis submitted in partial fulfillment of the requirements for the degree of
MS Mechanical Engineering

Thesis Supervisor:

DR. KHALID MAHMOOD

Thesis Supervisor's Signature:

A handwritten signature in purple ink, appearing to read 'Khalid Mahmood', is written above a horizontal line.

DEPARTMENT OF MECHANICAL ENGINEERING
COLLEGE OF ELECTRICAL AND MECHANICAL ENGINEERING
NATIONAL UNIVERSITY OF SCIENCE AND TECHNOLOGY,
RAWALPINDI
SEPTEMBER , 2020

Declaration

I certify that this research work titled “*Modeling of the effect of non-spherical particles of various sizes using Direct Laser Deposition (DLD)*” is my own work. The work has not been presented elsewhere for assessment. The material that has been used from other sources it has been properly acknowledged / referred.



Signature of Student

NS MURSALEEN SHAHID

00000204954

Plagiarism Certificate (Turnitin Report)

This thesis has been checked for Plagiarism. Turnitin report endorsed by Supervisor is attached.



Signature of Student
MURSALEEN SHAHID
Registration Number

00000204954



Signature of Supervisor
Dr. Khalid Mahmood

LANGUAGE CORRECTNESS CERTIFICATE

This thesis has been read by an English expert and is free of typing, syntax, semantic, grammatical and spelling mistakes. Thesis is also according to the format given by the university.



Signature of Student

NS MURSALEEN SHAHID

Student ID:00204954



Signature of Supervisor

DR. KHALID MAHMOOD

Copyright Statement

- Copyright in text of this thesis rests with the student author. Copies (by any process) either in full, or of extracts, may be made only in accordance with instructions given by the author and lodged in the Library of CEME NUST.
- Details may be obtained by the Librarian. This page must form part of any such copies made. Further copies (by any process) may not be made without the permission (in writing) of the author.
- The ownership of any intellectual property rights which may be described in this thesis is vested in DME CEME NUST, subject to any prior agreement to the contrary, and may not be made available for use by third parties without the written permission of the DME, which will prescribe the terms and conditions of any such agreement.
- Further information on the conditions under which disclosures and exploitation may take place is available from the Library of CEME NUST Rawalpindi.

Acknowledgements

First of all, I am grateful to ALLAH, who has given me guidance, strength and enabled me to accomplish this task. The journey on this road of success had not been possible without His will, and henceforth, all this success and accomplishment, I owe it to Him, in totality.

I want to thank my Parents for their support and prayers. They have been a driving force and without their support I might not have been able to get done with my thesis. I am grateful to my siblings, friends and well-wishers for their untiring support.

I would like to express gigantic gratitude to my supervisor Dr Khalid Mahmood, for his help and motivation throughout this journey of completing my research work. Without his help I would have not been able to accomplish this tedious job. Under his guidance, I am able to achieve my goals. He helped me throughout this journey of research and I'm really grateful for his unfailing support and assistance throughout my work.

I would like to thank my GEC member Dr Nadeem Sheikh for his willingness to offer me his precious time and intellect during my research.

I would like to thank my GEC member Dr Tariq Talha, for broadening my concepts and guideline about research outline.

*Dedicated to my exceptional parents and adored siblings whose
tremendous support and cooperation led me to this wonderful
accomplishment.*

Abstract

Additive manufacturing (AM) is the identical name to describe the new creation of manufacturing technology that built 3D objects by adding materials in layers, whether the material is in plastic, ceramics, metal and or it is advancing towards human tissues. AM can also be described as rapid manufacturing (RM). AM processes needs only few basic dimensional details, understanding of AM machines and building material that could be used to manufacture the part. Direct Laser deposition (DLD) is form of AM, a method that has a great possibility to reduce material waste through near net shape production in addition to increasing value to a previously manufactured pricey module (aviation and aerospace industry. Direct Laser deposition (DLD) process offers the potential to make a metallic component directly from CAD file. The focus of this study is an investigation of powder stream process, a sub process of DLD. Powder stream and processing parameters are highly important in clad formation, it directly affect powder distribution, temperature attenuation of beam and velocity during DLD. Various Modeling techniques have been used to model this sub process but in this work discrete element method using Lagrangian-Eulerain approach has been used and a review of analytical Modeling has been done. Effect of different processing parameters on clad height has been studied. The results of these investigations have also been validated with an experimental work.

Key Words: *DLD, LE, DEM , additive manufacturing*

Table of Contents

Declaration	i
Plagiarism Certificate (Turnitin Report)	ii
Copyright Statement	v
Acknowledgements	vi
Abstract	viii
Table of Contents	x
List of Figures	xii
List of Tables	xiv
CHAPTER 1: INTRODUCTION	1
1.1 Background	1
1.1.1 Lagrangian-Eulerian Approach	3
1.2 Literature Review	4
1.2.1 Additive Manufacturing	4
1.2.2 Direct Laser Deposition.....	6
1.2.3 DLD Process Description	7
1.2.4 DLD Processing Features	8
1.2.5 Processing Parameters	9
1.2.6 Effect of Processing Parameters	10
1.2.7 DLD Applications.....	11
1.2.8 Modeling Details	12
CHAPTER 2: Modeling Technique	18
2.1 Introduction:	18

2.2. Solver.....	18
2.3. Governing Equations	19
2.4. Difference between Dilute and Dense Flows	22
CHAPTER 3: POST PROCESSING	32
CHAPTER 4: RESULTS AND DISCUSSIONS	48
SUMMARY	49
Conclusion and Future Suggestions	50
REFERENCES.....	51

List of Figures

Figure 1 Block Diagram.....	4
Figure 2 Selective Laser Sintering.....	5
Figure 3 Direct Laser Deposition.....	6
Figure 4 Melt Pool Shape Parameters.....	8
Figure 5: Mesh of Different sizes to measure particles	10
Figure 6: Diagram of two particles in contact	14
Figure 7: Multiphase Model Flow Chart	18
Figure 8: Discrete Element Method (DEM)	19
Figure 9: Volume fraction.....	19
Figure 10: Volume Fraction effect on packing of particles	20
Figure 11: Dense Flow Classification.....	23
Figure 12: Meshing.....	26
Figure 13: Volume Fraction.....	27
Figure 14: Density representation in MFix.....	28
Figure 15 Velocity	28
Figure 16: DEM Settings	28
Figure 17: Particle Generation	29
Figure 18: Euler method for integration	29
Figure 19: Collision Model.....	29
Figure 20: Coupling Method.....	29
Figure 21: Interpolation in MFix	30
Figure 22: Interpolation Scheme.....	30
Figure 23: Fit particles MFix	30
Figure 24: Radiation Temperature	31
Figure 25: ESP Movement through Nozzle	32
Figure 26: Temperature Distribution at 0.05s.....	33
Figure 27: Temperature Distribution at 0.08s.....	33
Figure 28 (a): Temperature Distribution at 0.12s	34

Figure 29 (a): Temperature Distribution at 0.16s	35
Figure 30 Temperature Distribution at 0.34s	36
Figure 31 Temperature Distribution at 0.4s	36
Figure 32(a): Temperature distribution at 0, 0.1s	37
Figure 33(a) : Temperature Distribution at 0.28s	38
Figure 34: Particle Drop through nozzle exit.....	40
Figure 35: Particle entering the bed	41
Figure 36: Layer Formation	42
Figure 37: Layer Formation	43
Figure 38: Mass flow rate vs layer height of small shavings at 800W	44
Figure 39: Mass Flow rate vs layer height at 1000W	45
Figure 40: Mass flow rate vs Layer height of large shavings at 800W	46
Figure 41: Mass flow rate vs layer height of large shavings at 1000W	47

List of Tables

Table 1: Equivalent Spherical Diameters	16
Table 2: Physical Properties.....	23
Table 3: Physical Properties.....	24
Table 4 Physical Parameters of System.....	24

CHAPTER 1: INTRODUCTION

1.1 Background

Direct Laser Deposition (DLD) is a category of additive manufacturing method which allows elements of required shape to be constructed using 3D CAD patterns [1]. DLD constructs the part layer by layer, unlike conventional machining where material is separated to generate the anticipated structure. A laser in DLD is used to generate a melted liquid, to which the robust stuff is added in the form of supply of metal powder. Where solid particles are added to the molten pool after passing through laser, a tiny droplet comprising of molten material is produced. With time both the heating source and solid material input shift away, the melt pool tracks the heating source permitting the earlier formed melt pool to freeze. Heating source in the form of laser and non spherical powder inputs are then shifted in the vertical direction and the next layer of the geometry under consideration is dumped over it. Progressing in this way, parts of complex geometry are manufactured.

It is crucial in many of production process, to produce classy complex parts. In the DLD process, it includes dimensional precision in addition to suitable molten material characteristics. The dimensional precision and microstructure features are well-defined by melt pool morphology and melt pool temperature, correspondingly.

Thus, in order to build parts with hand specified dimensions or chosen microstructure features, a closed-loop process controller should be applied. Using a prototype of the DLD process that combines height dependence allows for the control multi-layer depositions.

Since DLD involves multiphase flow is a simultaneous flow of materials with

- Different phases like solid , liquid or gas.
- Different chemical properties but within the same phase properties like liquid-liquid flows such as oil droplets in water.

In multiphase flows like gas-solids area unit particularized not solely in many engineering processes, comprising energy sector, chemical, pharmaceutical, food, and agriculture process sectors, however conjointly in several natural phenomena, like sandstorms and cloud particles. to enhance the look and development of commercial methods and to precisely account for the natural phenomena that involve multiphase flows, an in-depth consideration of gas–solids flows is desired. With the invention of high-speed computers and

procedure algorithms CFD modeling has come to be a crucial means to assist accomplish this goal [2].

Two main techniques to simulate gas-solid flows are [3] :

- Eulerian- Eulerian (EE)
- Lagrangian-Eulerian (LE)

In Eulerian-Eulerian technique both phases are taken as interpenetrating continuum. This involves conversion formulas of change in energy, momentum and mass for separately individual phase, also fluid phases are derived through average method. This process delivers us unfamiliar terms that need conclusion models for example drag force, stresses. In order to obtain constitutive relationships for the solids phase condensed gas kinetic theory is repeatedly using [4],[5]. However, various empirical relationships have also been proposed for this determination [6], [7].

However, For the interpretation of forces occurring during collision of particles and forces exerting on the particles by the gas phase are solved in Lagrangian–Eulerian approach (LE) for each discrete particle or group of particles, Newton's laws of motion is used. Besides these CFD developing techniques, many other approaches are also helpful such as Discrete Bubble model (DBM) or direct numerical simulation (DNS) and lattice-Boltzmann method (LBM) can be originate from the literature [8].

Both EE and LE approaches has its benefits as well as drawbacks. For instance, the Lagrangian- Eulerian method is quite simple than the Eulerian-Eulerian technique for developing solids with changed particle physical properties like size, temperature ,density etc., however, it is not yet possible, even with super computers, to simulate a large-scale system due to the massive computational expense of tracing each particle.

In a particle-fluid flow, momentum conversation as a result of change in phase shows a crucial function in the varying aspects of element movement and interaction [9],[10]. The approach wherein this term is processed varies with the chosen multiphase illustration, which can be termed as either Eulerian–Eulerian (EE) or Lagrangian-Eulerian (LE) [11].

In the earlier one, the distinct parts of flow are supposed to be inter-penetrating scales. As for each phase there is a consideration of a continuum description, comprising of a equations of conservation of masses, momentums and energies and in constitutive equivalences interphase momentum exchange is explained.

1.1.1 Lagrangian-Eulerian Approach

Lagrangian–Eulerian (LE) method is used to determine the properties of multiphase flows such as particle–laden or in case of spray streams used in numerous energy products. LE method is used in a family of multiphase flow analysis and simulation techniques in which particles are dropped through the nozzle that are characterized in a Lagrangian frame of reference while the carrier phase flow is characterized in a Eulerian .

For any simulation approach for instance the LE method to be used as an analytical tool, it must be based on:

- a numerical interpretation that can represent the physical trends of concern [12].
- precise and reliable prototypes for the unclosed standings that need to be shaped.
- a statistically steady and convergent execution.

There are faces in each of these sections that must be conquered for a development of such a prognostic LE approach model procedure for multifluid flows. Another benefit of the LE method above the EE approach of two–phase theory is its capacity to precisely measure impact of collisions between particles in the existence of flow. It is well known that connections with the ambient flow can substantially modify the collision attributes in particle–loaded or droplet–loaded flow (grazing collisions), and the active restitution coefficient is a function of the particle or droplet Stokes number [11].

In DLD process, inert gas delivers shielding to reduce oxidation. Researchers have used Argon, Nitrogen and Helium for this purpose.

DLD processes have an aim to generate 3D end products. Stable powder material in molten pool may be used for parts of production. Material is used in form of powder as well as wire but powder is usually preferred form. It has benefit of regulating the clad dimension. Generally, in DLD process metals like aluminum alloys or gold having high thermal reflectivity as well as thermal conductivities are not easy to process. Metallic materials with good weldability quality can be processed reasonably. Powder refers to processed from of ceramics as well as metals. grinding. Further, DLD also employs Gas atomized (GA) metal powder to produce powder particles of spherical shape.

These properties are effortlessly integrated using LE technique. Likewise, from a statistical point of view, the LE method of multiphase is used to lessens statistical dispersion in discrete–phase fields such as mean velocity of each phase and volume fraction when associated to grid–

centered Eulerian method. CFD analysis using LE approach is briefly explained by using the following diagram.

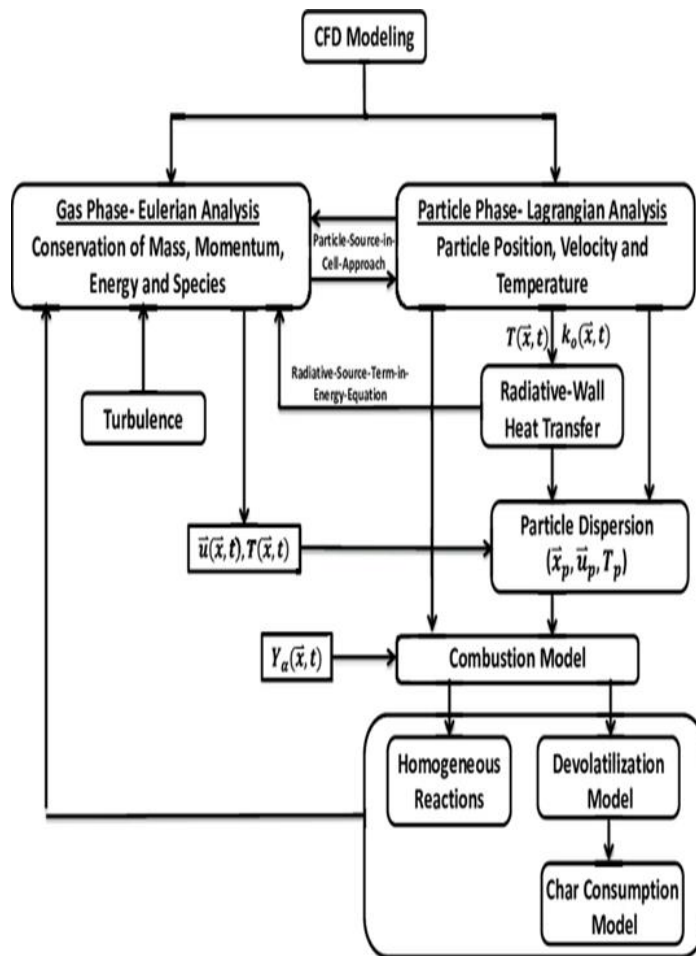


Figure 1 Block Diagram

1.2 Literature Review

1.2.1 Additive Manufacturing

Additive Manufacturing (AM) is picking up consideration from later a long time due to expanded mechanical advancement and diminishment in time and exertion. AM allows direct adaptation of build design files into fully functional bits and pieces. Using additive tools, objects from metals, plastics, ceramics, glass, sand and other materials are build up in layers until unless they achieve their final shape [13].

Depending on the material used during 3D printing, specific type of binder system or laser technology are used in order to bind the particles as well as layers with the aim of achieving the required shape. Additive Manufacturing is now playing a key role in medical and

orthopedic fields[14].

Unlike to a material subtraction process like in CNC machining AM is a 3D process of layer by layer material addition process using heat source, how much complex the geometry is, AM can make this easily. Additive Manufacturing involves various techniques regardless of typical feature of layer by layer addition of materials. One of its basic technique is consist of powder already present on bed and production of part takes place through selective laser sintering (SLS) process. In another technique metallic powder can be injected through laser metal deposition (LMD), sometimes called Direct Laser Deposition (DLD). LMD is the main technique of AM where powder becomes in contact with laser beam while deposition, melting the material with the aid of laser power and making a melt pool on the substrate.

Both Selective laser Sintering (SLS) and a Direct Laser Deposition (DLD) processes are illustrated in Fig 2 and 3 respectively.

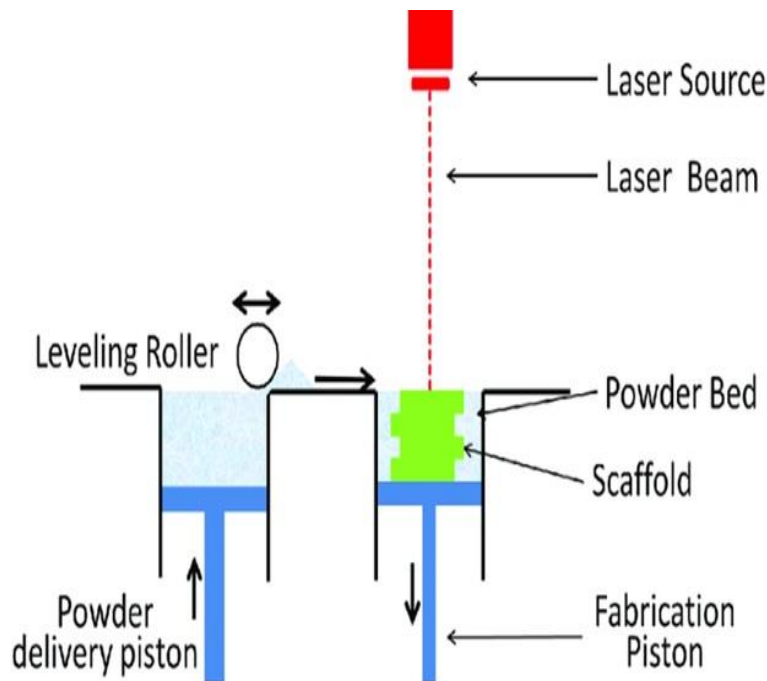


Figure 2 Selective Laser Sintering

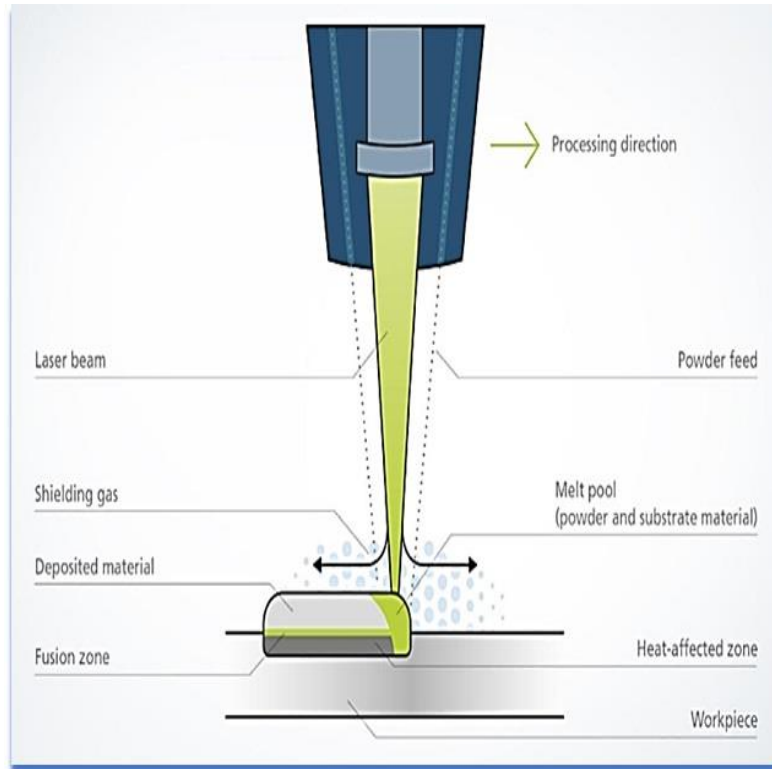


Figure 3 Direct Laser Deposition

The overall examine of AM process are as follows:

- Making a CAD file in computer
- Convert this file into STL format
- Transfer the file into AM Machine in the form of G-code
- Setup of AM Machine
- Building of Part
- Remove part from machine
- Post Processing of the built component
- Application

1.2.2 Direct Laser Deposition

The DLD process is vigorously complex and usually need comprehensive and much difficult models, whose geometry is not easy to make through conventional process, to elaborate the relationships among various process inputs as in this case is laser power, mass flow rate of particles in the presence of gas, scan speed and the physical measures of concentration, which comprise the temperature and dimensions of melt pool.

DLD process allows the formation of component by melting the material first as it is being

dumped through some deposition head. This process is very much suitable for ceramics, polymers as well as metal composites but is preferred for metallic powders.

1.2.3 DLD Process Description

Direct laser deposition (DLD) is a comprehensive process that is governed by using mass, fluid and thermal analysis of flow [15]. As various complex interactions are used to form the molten fluid morphology, where many of the results shows that the molten substrate takes the form of half of the ellipsoid [16]. Where, the principal axes of the plane molten substrate are the shape parameters i.e. width and length parameter height are obtained through vertical half axes.

So, the volume in addition to the area obtained in the direction of deposition are as follows.

$$v_i = \frac{\pi}{6}(w)(h)(l)$$

$$A_i = \frac{\pi}{4}(w)(h)$$

Where,

v_i = volume of melt pool in m^3

w =width of the melt pool in m

h =height in m

l =length in m

Usually the face of the molten substrate is assumed to be placed at the identical position as the laser thus, one can measure the length of the molten substrate by using the following equation:

$$l_i = d_i - s_i$$

Where,

d = position of laser in meters

s = solidification front in meters

l = length of the melt pool

By using above equation, the part obtained using laser beam and flow rate above the substrate are stationary system. And the solidifies region obtained by using solidified material consist of two portions. One of it is for a wafer-thin hedged piece, the layer will have the length L_t as out of layer length and in layer solidifies material has length s that solidified as shown in figure below.

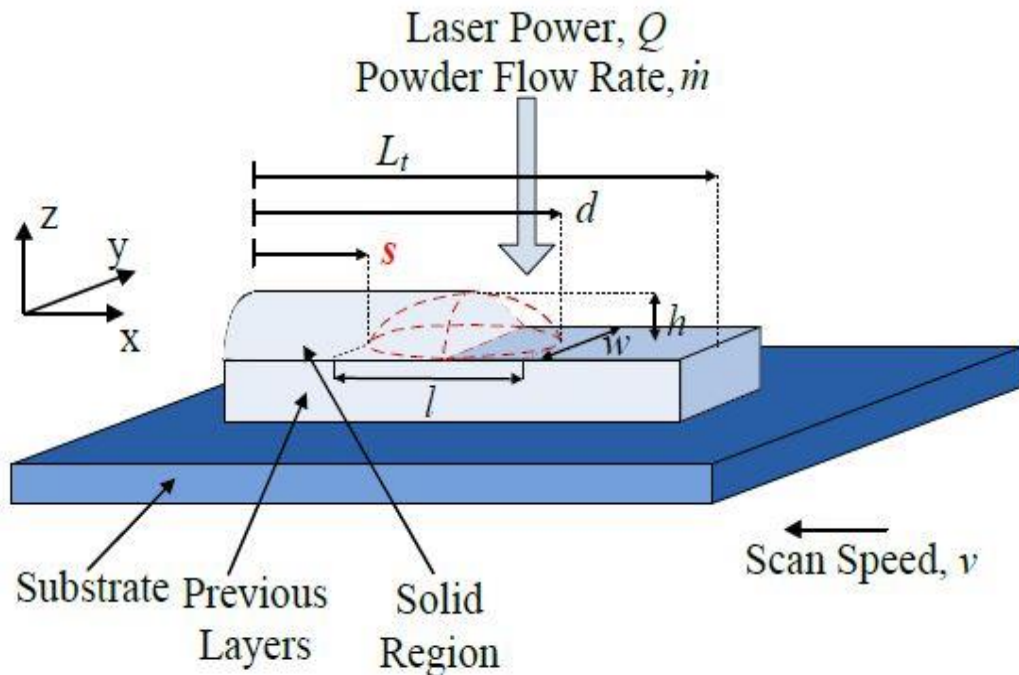


Figure 4 Melt Pool Shape Parameters

1.2.4 DLD Processing Features

DLD processes aim to create 3D end products. Powder, which is stable in the molten pool, can be utilized for the production of parts. Material used in DLD process can be in the manner of wire or in some cases powder, but powder is generally a best choice. One of the main advantages of DLD process is to adjust the clad dimensions as required. Usually metals with high thermal conductivities and reflectivity like gold and aluminum are difficult to deal with DLD process [1].

Metallic Materials with good welding capability are reasonable to process with DLD. Powder is usually processed from metals and ceramics. Ceramics powders are mostly produced by crushing and grinding. Gas atomized (GA) metallic powders has been in use when it comes to

DLD as it produces spherical shape particles [17]. Another cheap method for producing powder particles is water atomized particles but there is a chance to deviate from their regular spherical shape [18].

1.2.5 Processing Parameters

Following are the important factors that greatly affect the properties of Direct laser deposition (DLD) process.

- Mass Flow Rate of Powder
- Laser Power
- Diameter of Beam

Mass Flow Rate of Powder

The quantity of material delivered per unit time. It greatly influences dimensional accuracy of the deposited layer including mechanical properties of the final products [19].

Laser Power

The source of energy required to melt the material in a powder or wire form and greatly influence the dynamics of the melt pool. Different laser types are used in DLD process with varying wavelength as laser power increases absorption of energy for most of the metal decreases [20].

Diameter of Beam

It determines the spot diameter of laser that consequently tells the width of the deposited layer [21].

Many other parameters accounted for DLD process are as follows:

- Geometry of Nozzle
- Carrier gas flow rate
- Injection angle
- Standoff Distance
- Powder feed rate
- Preheating process of the powder

1.2.6 Effect of Processing Parameters

Powder Size and Morphology

Main features of the powder particles are as follows:

- Particle size
- Particle shape

Particle size involves dimensions of individual particles. In order to measure particle size various methods can be used. Most common method uses screening of different mesh sizes [22] as shown in figure 5. Measuring the particle size using filtering or sieving is one of the traditional method to calculate size of the particle. Depending on the mesh size particle sizes can be determined.

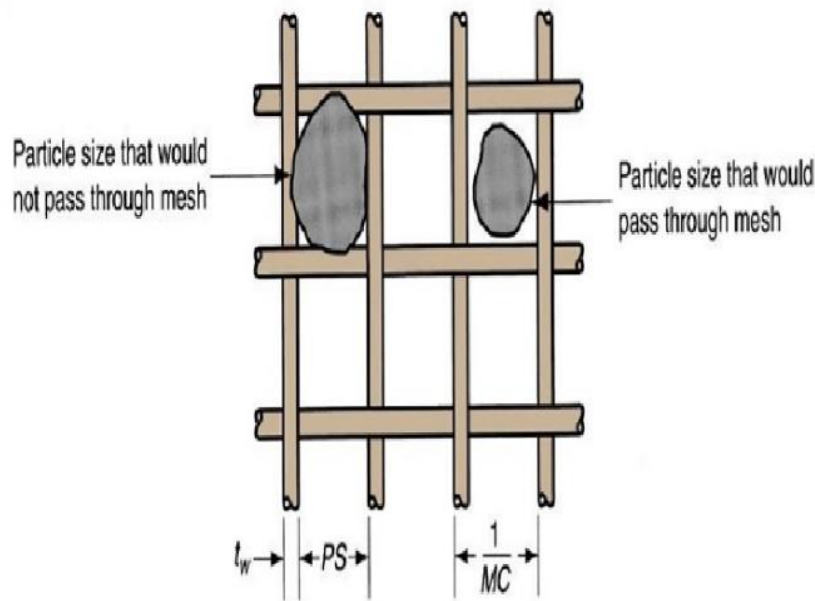


Figure 5: Mesh of Different sizes to measure particles

Particle size can be measured using following equation

$$\text{Particle Size} = PS = 1/MC - tw$$

Where MC is the mesh count and tw is the wire thickness of the screen mesh. Besides this method, microscopy and X ray diffraction [23] technique can also be used. Dimensions of

various particle shapes can be described in terms of spherical and equivalent spherical particles for non-spherical shapes.

Spherical Particles can be measured directly from diameter of the particle. While for non-spherical particles aspect ratio is used to measure the approximate results. Particles are mostly categorized into spherical particles, near spherical and non-spherical shape of particles.

Particles size and shape performs an essential role in DLD process in terms of deposition quality and deposition efficiency. It has been observed that quality of the final deposited layer is totally dependent on shape of particles. As the particle size increases, it weakens the consistency of laser power and energy degradation occurs [24].

1.2.7 DLD Applications

Research have been carried out broadly in AM and concisely in DLD process and it indicated a broad selection of applications. Main reason behind this research is the flexibility in different processing parameters that are difficult to machine and building end products having complex shapes. DLD does not cost the complexity of design. Some of applications has been found as below:

- Repair and production of components for aeronautics and aerospace industries [25].
- Instruments maintenance/ Repair and reestablishing of tools [26].
- Cladding by DLD process [27].
- To increase the structural properties of parts for example hardness, fatigue and yield strengths [28].
- This process can be used where less heat effected zones are necessary [29].
- Building smart components [30].
- Thermal Spraying and Electroplating [31].
- In medical, creation of surgical instruments and implants [32].

Various Modeling techniques have been used to model this process sub process such as:

- Statistical Modeling
- Dimensional Modeling
- Analytical Modeling

The approach we use here is the statistical modeling technique where LE approach is used using Discrete Element Method.

Gas and solid flows are not only participating in various industrial process but also includes in various processes naturally including sandstorms and cosmic dusts.

Two most common methods used to reproduce gas solid fluid flows are:

- Eulerian-Eulerian Method (EE)
- Lagrangian-Eulerian Method (LE)

In Eulerian-Eulerian (EE) method, every part of multiphase flow is considered as interpenetrating continuum and the values for the conservation of energy, momentum and mass are derived for both the particle and fluid phase. Using this process, we can find unknown terms which are involved in closure models like stress, drag. While in (LE) approach, forces arising during particles collapse and also the forces arises on the particles by liquid or gaseous phase are solved using Newton`s laws of motion for counting the forces for each individual particle and Navier Stock equation is used to find the unknowns in continuum phase of gaseous particles.

Both above methods have certain advantages and disadvantages, just like LE method is quite simple and straightforward as compared to EE approach for modeling solid phase analysis with different particle properties like height, density etc.

1.2.8 Modeling Details

The approach we are using here is LE approach which uses Discrete Element Method (DEM), a technique used over the past 30 years. It is a numerical method used to calculate interaction of small particles in a large number.

For particle flow models, this process estimates displacements and rotation of various type of particles. When this technique is used for solving microparticles, interconnected forces like in our case Van der Waals forces are not performing a big role in how particle structures pack collectively. The distribution of particle size inside the shavings or powder scheme is the most useful aspect in defining how the particles are packed collectively.

Computational Fluid Dynamics (CFD):

In fluid mechanics, a very large subfield is computational fluid dynamics. This is the area of skill where numerical solutions of fluid glitches are solved. The problems studied here tend not to be solvable with an analytical approach, so a purely numerical solution is estimated. The

domain to be computed is known as the control volume (CV) and this stretches over the body and encasing surroundings as well. The difference between control mass (CM) and control volume is that in the case of mass, the system follows the matter, whereas with a control volume, the volume stays the same, but the mass flows through. This volume is then split into discrete parts for possible computation, this is known as discretization and are later needed for the finite volume method.

Discrete Element Method (DEM):

In this approach, particles of diameter D_m where, m is the indication of m th solid phase, number of particles N_m , and density $\rho_s m$ are used to characterize microparticles flow. Total number of particles is obtained by each equivalent spherical particle overall number of solid phases, M , as given by Equation.

$$N = \sum_{m=1}^M N_m$$

In this equation, N particles is defined within a Lagrangian reference at time by its position, velocity, angular velocity, diameter, density and mass. Both the linear and angular velocities are obtained used Newtons laws as mentioned below.

$$\frac{dX^{(i)}(t)}{dt} = V^{(i)}(t)$$

$$m^{(i)} \frac{dV^{(i)}}{dt} = F_T^{(i)} = m^{(i)} g + F_d^{(i)}(t) + F_c^{(i)}(t)$$

$$I^{(i)} \frac{d\omega^{(i)}(t)}{dt} = T^{(i)}$$

Where X indicate position of particle at time in seconds t , linear velocity is denoted by V at that time of i th particle, $\omega^{(i)}$ is the angular velocity, F_d is a force created as a result of drag between particles, is achieved by summation of all the pressures and viscous forces. F_c is the force exerting on the particle when particles are in contact.

Inter-particles Contact Forces

For a contact forces, spring dashpot model is used in this analysis, which comprised on soft sphere model of particles and is applied for particles interaction. It is also used for calculating

contact between two micro scale particles to how much extent, as it has no restriction for multi particle contacts. Contacting force between particles is obtained by using equation

$$\delta_n = 0.5(D^{(i)} + D^{(j)}) - (x^i + x^j)$$

and when one particle is in line of contact with other particle, unit vector is given by equation

$$\eta_{ij} = \frac{(D^i + D^j)}{|x^i + x^j|}$$

Where, in equations above for the soft sphere collision shown in figure 6, two particles i and j of diameter $D^{(i)}$ and $D^{(j)}$ are located at position $X^{(i)}$ and $X^{(j)}$ moves with linear velocity V and angular velocity ω .

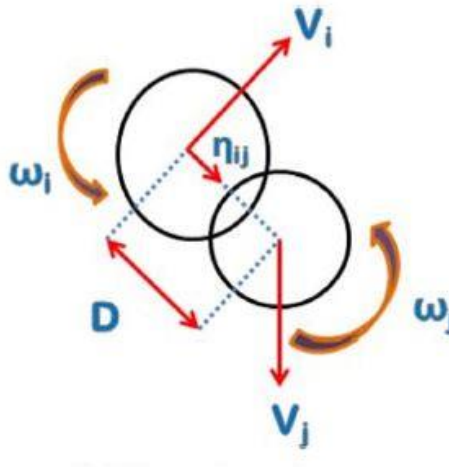


Figure 6: Diagram of two particles in contact

The heat distribution is implemented by linking heat conduction over the particle contacts and heat creation due to laser heat source. So, the laser is set up with specific power Q .

$$Q = kA\Delta T$$

Where, heat transfer coefficient is represented by k . Above equation is used to determine the laser power Q . While for the point of contact between two particles i and j , relative velocity is given by

$$V_{ij} = v^i - v^j + (L^i \omega^i + L^j \omega^j) \times \eta_{ij}$$

Where L indicate distance of contact points from the center of particles i and j .

In this paper, a soft sphere model used for the overlap between two adjacent particles is presented by system of spring and dashpots. In spring and dashpot system of contact force, springs are utilized to show the elastic interaction between every contacting particles while the effect of dashpots are used to represent the loss as a result of kinetic energy due to inelastic collision. The stiffness of the springs is mentioned both in normal and tangential directions. There stiffness is dependent upon the elastic module of the particles at the time of interaction. Similarly, dashpot damping coefficient is provided to every single particle collaboration both in the normal and tangential directions is resolute by inelastic dispersion of particles collision. Relationship between dashpot coefficient and coefficient of restitution:

Correlation of normal coefficient for dashpot and normal restitution coefficient is given by equation:

$$\eta_{m_i} = \frac{\sqrt{m_{eff} k_{nm} |lne_{nm}|}}{\sqrt{\pi^2 + lne_{nm}^2}}$$

Where normal dashpot coefficient is η gives us the relation with normal restitution coefficient. And the normal damping coefficient is twice of the tangential damping coefficient. Consequently, the normal coefficient of restitution matrix and tangential restitution coefficient are written as N x N matrices that is symmetric for N solid phases as shown below.

$$[e] = \begin{bmatrix} e_{xx} & e_{xy} & e_{xz} \\ e_{yx} & e_{yy} & e_{yz} \\ e_{zx} & e_{zy} & e_{zz} \end{bmatrix}$$

Cohesive Forces:

Interaction between two particles that are in contact and cohesive forces generated between particles and walls interaction are modeled using Derjaguin-Muller-Toporov (DMT) model. Where the cohesive forces are considered by applying the inner and outer cutoff value of the particles and the walls as mentioned in equations below

$$F = 2\phi R \left(\frac{h}{h+R} \right) + \left(\frac{1}{\left(1 + \frac{h}{r}\right)^2} \right)$$

$$F_{inner} = 2\pi\phi R \left(\frac{h}{h+R} \right) + \left(\frac{1}{\left(1 + \frac{h}{r_{inner}}\right)^2} \right)$$

Where the equivalent spherical Radius is represented by R separation distance is denoted by r , surface energy is indicated by ϕ , r_{inner} is inner cutoff cohesive value between the particles, h is the asperity defines the impurity and roughness on the surface. The surface energy ϕ is given by

$$\phi_i = \frac{A_i}{24\pi D_0^2}$$

Where cutoff distance is shown by D_0 and is the same to r for surface energy and A is the Hamaker constant.

Particle Size Distribution:

In this analysis, the particle size is uniform. Values are taken at various equivalent spherical diameters for non spherical particles of sizes 86.8 μ m and 199.3 μ m as shown in Table 1.

Table 1: Equivalent Spherical Diameters

Particle Type	Mean Equivalent Spherical Diameter ESD*(μ m)
Small Shavings	86.8 μ m
Large Shavings	199.3 μ m

Porosity:

Pore and void formation is divided further into categories in process of laser metal deposition and named as:

- Inter-layer
- Intra-layer porosities
- Inter-track

Inter-track:

Inter track voids created by offset tracks or also by horizontally aligned aspect ratios. Deposited molten base does not adhere to substrate of deposited material and hence bubbles are generated near base.

Inter-layer:

Inter layer flaws are generated due to less fusion of vertically aligned deposition. There are many factors which may be the reason of this lack of proper fusion and include inconsistent energy, misplaced tracks and oxide layers.

Intra-layer:

Intra-layer porosity occurs in spherical areas in a layer. It is described in laser metal powder deposition via trapped gas among the powder particles. While, laser welding also found that voids may also be generated through moisture which exists in industrial-grade shroud gases. When power is increased, material vaporization may occur as problem.

Particle-fluid interactions

Four techniques are used in simulations of flow of particle. Techniques chosen depend on degree of dispersity specifically in multiphase flow. More bubble fluid is necessity for interaction of particle-particle in solver. It is not important for the dilute concentrations and only proceeds with the processing time. Four techniques are briefly described below:

One-way coupling:

Flow effects the particles movement. Particles show movement with same velocity in fluid and at the same time fluid is not affected by these particles. Particles get effected by buoyancy in this model, and buoyancy may cause particles to float or sink due to their mass.

Two-way coupling:

In this model, flow effects the particle movement and flow is also effected by particles existence. This means that fluid flow may get changed due to particle disturbances. Further, buoyancy effects may also cause feedback due to turbulence damping.

Four-way coupling:

It is almost same as is two-way coupling with only difference that here additional interaction is observed between particles as fluid streamlines are usually compressed between different particles and particle-particle interaction. Hence, it may increase the possibility of collision and presence of friction.

CHAPTER 2: Modeling Technique

2.1. Introduction:

Multiphase flow is involved in this process where one of the phase is primary called continuous while other is called secondary phase which is dispersed within continuous phase where diameter is assigned to each secondary phase. Eulerian-Lagrangian and Euler-Euler are two approaches which are further classified. The approaches used in any multiphase model is explained by figure 7.

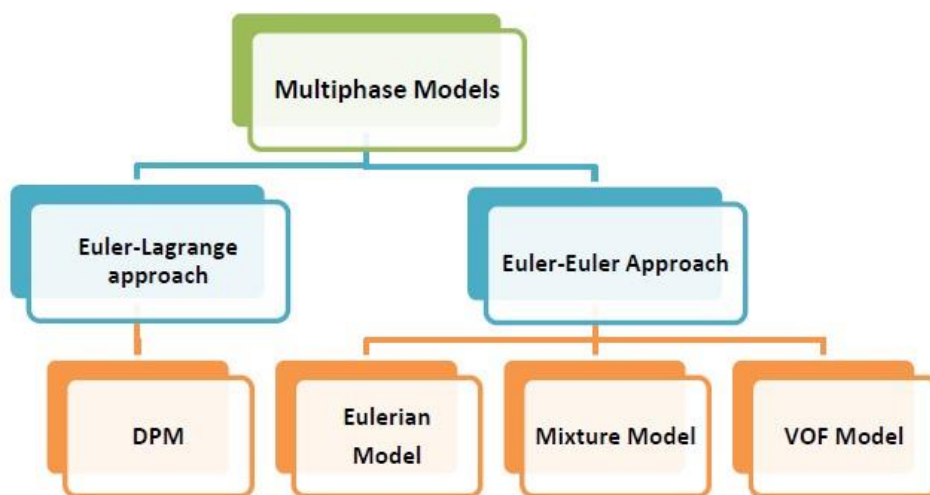


Figure 7: Multiphase Model Flow Chart

Where Discrete Particle method sometime called Discrete Element Method is used here in this process. This technique has been under consideration of many researchers since the inventions of DLD process. Modeling is performed usually to predict the results without performing the physical phenomenon. To compute this computational technique, we use MFix Software, an open source multiphase flow solver.

2.2. Solver

In this process Discrete Element Model solver is used which uses Lagrange Eulerian (LE) approach as shown in figure.

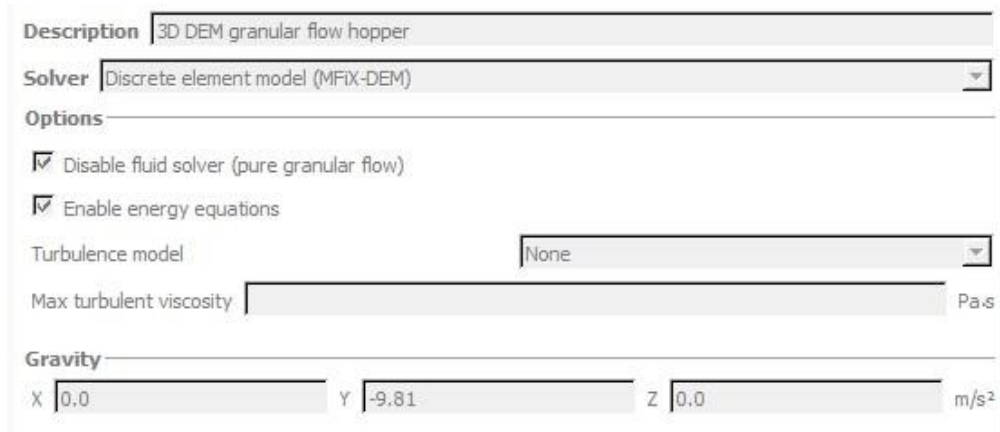


Figure 8: Discrete Element Method (DEM)

In figure 8, the solver is MFiX-DEM and the factor of gravity is introduced here. As the particles are falling downward due to gravity so value of gravitational acceleration is introduced in y direction taken as -9.81.

2.3. Governing Equations

Using Newton`s Laws, the solid phase is demonstrated whose linear velocity, position and angular velocity is obtained. While the unsolidified phase equations are identical as EE version of MFiX. Volume fraction of the dispersed phase is explained in figure 9 and is defined as

$$\left\{ \text{Volume fraction of a phase} = \frac{\text{Volume of the phase in a cell/domain}}{\text{Volume of the cell/domain}} \right\}$$

Figure 9: Volume fraction

$$\varepsilon_{solid} = \frac{\delta v_{solid}}{\delta v}$$

Where, $v_{(sm)}$ is the solid phase volume in a cell and v is the cell volume. Also, volume fraction of the continues phase or fluid phase is:

$$\varepsilon_{fluid} = \frac{\delta v_{fluid}}{\delta v}$$

The sum of the volume fraction of the solid and carrier gas phase is equal to one.

$$\varepsilon_{fluid} + \sum_{m=1}^m v \varepsilon_{solid} = 1$$

Where, the volume fraction ε of different phases i.e. fluid and solid refer to the phases of both the fluid and solid and m is the number of m th solid phase where if more than one solid phase is present its sum will be equal to one. Figure 10 indicates the effect of volume fraction on particles packing that how close they are packed.

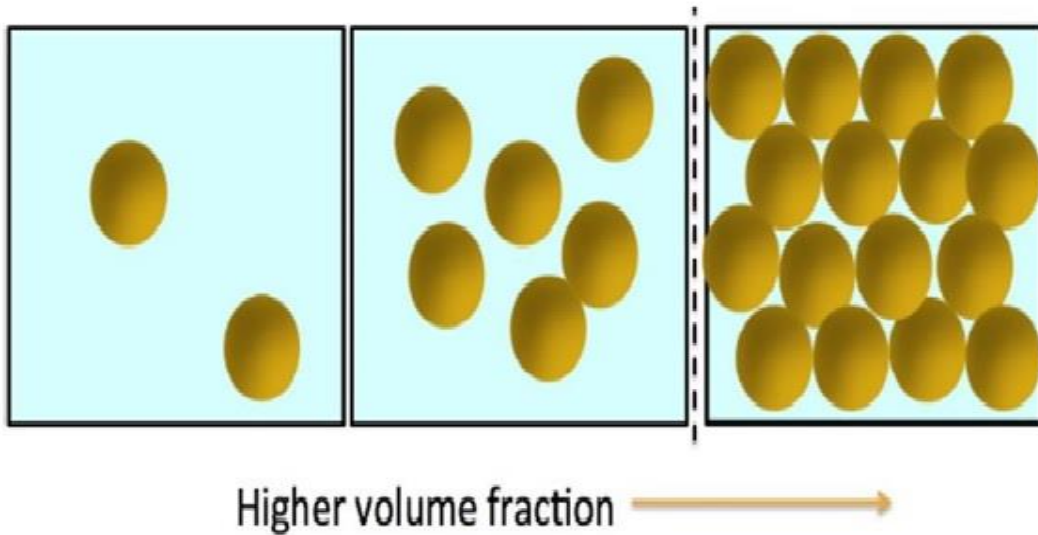


Figure 10: Volume Fraction effect on packing of particles

While the mass and the momentum equations for the fluid phase in the absence of change of phase are as follows:

$$\frac{\partial}{\partial t} (\varepsilon_{fluid} \rho_{fluid}) + \nabla \cdot (\varepsilon_{fluid} \rho_{fluid} \mathbf{v}_{fluid}) = 0$$

$$\begin{aligned} \frac{\partial}{\partial t} (\epsilon_{fluid} \rho_{fluid} v_{fluid}) + \nabla \cdot (\epsilon_{fluid} \rho_{fluid} v_{fv_{fluid}}) \\ = \nabla \cdot \overline{\overline{s_{fluid}}} + \epsilon_{fluid} \rho_{fluid} g - \sum_{m=1}^M \overline{\overline{I_{fm}}} \end{aligned}$$

In this equation ,

ρ indicates the density,

v is the illustration for velocity,

S_{fluid} = stress tensor for a fluid phase,

g = constant gravitational acceleration

and

I_{fm} is the value that represents the momentum transfer that is interphase between the phase of fluid and the m th solid phase.

The phase of the fluid can be regarded as an ideal fluid that is compressible and obeys the ideal law of fluid.

$$\rho_{fluid} = \frac{P_f M_w}{RT_f}$$

where

P_{fluid} = pressure of fluid,

M_w = molecular mass of fluid,

R = the universal gas constant

T_f = Fluid's temperature.

Although, MFI option allows the user to define the fluid phase as incompressible, by stipulating value of density to be set that is constant. The solid phase m th is characterized by N_{pm} spherically round particles and each one of the particles have density ρ_{sm} and diameter D_{pm} [32].

Total number of particles is obtained by

$$N_p = \sum_{m=1}^M v N_{pm}$$

where,

M = total number of solid phases.

The reference for the particles is taken as Lagrangian frame and with respect to time t by

$$\{x^{(i)}(t), V^{(i)}(t), \omega^{(i)}(t), D^{(i)}, \rho^{(i)}, i = 1, \dots, N\}$$

where,

X = ith particle's position

V = linear velocity

ω = angular velocities

D(i) = diameter

ρ = density.

For a particle fits to the mth phase of a solid, also its diameter and density are D_{pm} and ρ_{sm} , correspondingly. Mass of a particle is the product of its density and its volume (of the equivalent sphere):

$$m^{(i)} = \rho^{(i)} \frac{\pi D^{(i)3}}{6}$$

Also, moment of inertia is equal to

$$I^{(i)} = \frac{m^{(i)} D^{(i)2}}{10}$$

Both the linear and angular velocities are obtained used Newtons laws as mentioned before in the equations below.

$$\frac{dX^{(i)}(t)}{dt} = V^{(i)}(t)$$

$$m^{(i)} \frac{dV^{(i)}}{dt} = F_T^{(i)} = m^{(i)} g + F_d^{(i)}(t) + F_c^{(i)}(t)$$

$$I^{(i)} \frac{d\omega^{(i)}(t)}{dt} = T^{(i)}$$

Where X indicate position of particle at time t, V is the linear velocity at that time of ith particle, $\omega^{(i)}$ is the angular velocity, F_d is drag force, is obtained by summation of all the pressures and viscous forces. F_c is the force acting on the particle as a result of particles are in contact.

2.4. Difference between Dilute and Dense Flows

Dilute flow is the flow in which the particle motion is controlled by the fluid forces like lift and drag force effects. While the dense flow is one in which particle motion is controlled by

collisions. Dense flows are further classified as collision dominated flows and contact dominated flows.

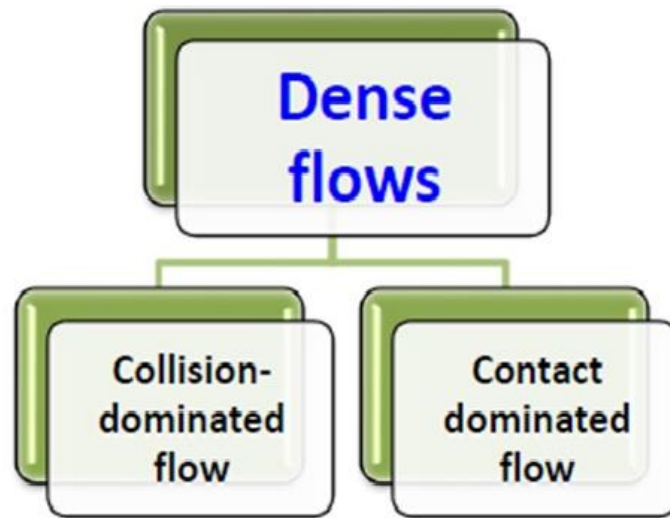


Figure 11: Dense Flow Classification

In collision dominated flows, there is a parameter of collision between the particles that is responsible to control the feature of flows. While in contact dominated flows, the particles motion is controlled by continuous contact as explained in case of shear granular flows.

Data:

Factors that can show variation during experiment are known as Effective variables such as mass flow rate power of laser and laser Power in this process.

Material

Stainless Steel 316L of different sizes are used for computation. Particle sizes of less than 150um was considered as small shaving (SS) and particles of sizes ranges from 150-250um was considered as Large Shavings (LS). Following are the physical properties of 316L stainless steel used in this work.

Table 2: Physical Properties

Notation	Physical Properties	Unit	316-L-Stainless Steel
Ts	Solid Temperature	[K]	1630
ρ	Density	[kg/m ³]	8000
Cp(solid)	Specific Heat of solid	[J/kg.K]	500
Hf	Heat of Fusion	[j/g]	260
ϵ	Emissivity		0.2

Shielding Gas

In this process, Argon (Ag) is used as a shielding gas to control the flow of depositing particles as well as to protect the optics from spattering.

Drag Model

The solver we used in this analysis is Discrete Element Method. While Gidsaspow Polydisperse drag model is used in this analysis. Various variable Process parameters are mentioned in table 3. and table 4 [33].

Table 3: Physical Properties

Parameter	Value
m Powder flow Rate (g/s)	0.12, 0.18,0.24,0.30
u Laser Scan Velocity (mm/s)	4
P Laser Power (W)	800,1000
d Standoff Distance (mm)	7.5
f Powder Density (g/mm ³)	0.008

Table 4 Physical Parameters of System

$r_{pinnercutoff}$ Minimum Inner Cutoff Particle Radius	40nm
$r_{poutercutoff}$ Maximum Outer Cutoff Particle Radius	500nm
Surface Asperity Size (h)	5nm
Wall inner Cutoff Value ($r_{winncutoff}$)	1 μ m
Wall outer Cutoff Value ($r_{woutercutoff}$)	5 μ m
Particle to Particle Spring Constant	10 ⁸ N/m

Particle to Wall Spring Constant	10^9 N/m
----------------------------------	------------

Geometry and Meshing

The geometry pane is used to describe the geometry. This actually includes whether the geometry is 2D or 3 Dimensional. The geometry section provides tools for adding geometry objects from STL or any kind of primitive elements. While all the geometry operations are done using Visualization Toolkit Library (VTK).

A three-dimensional geometry was used in this work. In this geometry we made rectangular box of dimensions 50x50x10 mm. The choice of 3D geometry was due to fact that at higher power levels, heat transfer in the third dimension was more significant [19]. While the flow of the particles is examined while falling from nozzle.

The meshing was done on MFix by the use of CutCell Mesher. The rectangular box was given length with one of its corner positions as the point of origin. The sides stretch according to the dimensions shown in table below. The geometry was chosen knowing that the laser beam in the laser metal deposition has a spot radius of 1.5mm.

The particles are dropped from nozzle in such a way that they are constantly dropped on the rectangular box and filled up all the space in the box on the assumption that both the box and the nozzle is stationary. The background mesh tab is used here for specifying the mesh used by Eulerian solver. A uniform mesh is specified by entering the numbers of cells in the x,y and z directions with the cells in x, y and z direction are of 50,100 and 50 respectively.

The indication of fine meshing is illustrated in figure 12.



Figure 12: Meshing

In order to simulate direct laser deposition, we need to follow these assumptions:

Initial temperature of the geometry is taken as 293K and laser, the geometry and the coordinate meshes were fixed. Particles from nozzle were dropped into the bed with the initial velocity set as 4mm/s and after the completion of one layer another layer was building over the first one and so on.

Boundary conditions applied to the deposited wall were as follows .

$$q_s = -h(T - T_0)$$

Also effect of radiation is also under consideration at that boundary condition so, radiative cooling effect is introduced in equation below

$$q = \sigma(T^4 - T_{\infty}^4)$$

Laser:

Effect of laser is introduced by using constant heat flux. The process was repeated for different laser powers i.e. for 800 and 1000 W. The heat transfer produced by the laser source was calculated via Equation.

$$Q = hA\Delta T$$

Where effect of heat measured is denoted by Q in [W], heat transfer coefficient denoted by h and is measured in [W/m².K], A is the area in [m²] also ΔT is the change in temperature measured in [K].

Sphericity:

It is actually the measure of how closely the object resembles to equivalent sphere.

Mass Flow Rate:

The simulation is done for different values of mass flow rates of powder i.e. 0.12, 0.18, 0.24 and 0.30. And different parameters are observed using these results.

Setting Solid phase Initial values:

Initial Values for solid field variables must be specified for the entire computational domain. The model being solved decree which variables require initial value.

Volume Fraction

Initially, the solid phase volume fraction has default value of zero. But in this process, we have assigned the initial value of volume fraction as 0.2. Such that, the sum of all the solid phases volume fractions are used to automatically calculate the volume fraction of fluid phases.

The solid volume fraction value is shown in figure 13.



Figure 13: Volume Fraction

Temperature:

The solid phase temperature has a default temperature of 300K. It is necessary when solving energy equation. While passing through the nozzle exit effect of laser is introduced due to which particles temperature starts changing according to laser power.

Defining Material Properties in MFix:

Few material properties are necessary for a specific solid model.

Software Settings:

- **Diameter:** It is the initial diameter of the particles and will remain constant for reactive as well as non-reactive flows with a variable density. For each case density will remain constant.
- **Density:** The particle density is taken as 8000[kg/m³]



Figure 14: Density representation in MFix

- **Velocity:** Velocity of 4mm/s is allowed to move particles from nozzle in -y direction as shown in figure 15.



Figure 15 Velocity

- **DEM Settings:** Using DEM tab specific DEM settings are accessed.



Figure 16: DEM Settings

- **Particle Generation:** Enable automatic particle generation. Using initial condition regions initialize particle location and velocity.

Enable automatic particle generation

Figure 17: Particle Generation

- **Integration Method:** While integrating particle trajectories, the Euler DEM time stepping scheme is used.

Integration method Euler

Figure 18: Euler method for integration

- **Collision Method:** Linear Spring dashpot, a soft spring collision model is used in this process.

Collision model Linear spring-dashpot

Figure 19: Collision Model

- **Coupling Method:** A fully coupled level of coupling is introduced between the gas and the solid phase.

Coupling method Fully coupled

Figure 20: Coupling Method

- **Interpolation:** A field to particle and particle to field is the interpolation technique that is used for direction of interpolation between field and particle data.



Figure 21: Interpolation in MFix

- **Square DPVM (Divided particle Method Scheme) interpolation scheme** is used in this process that requires an interpolation width.

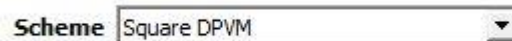


Figure 22: Interpolation Scheme

- **Friction Coefficient:** Friction Coefficient for both particle-particle and particle-wall are set as 0.4 each. This is required for both LSD and Hertzian Collision Models.
- **Restitution Coefficient:** The value of restitution coefficient is taken as small as we can so that the particles will no bounce back once it falls from nozzle exit. Its value is taken as 0.01. for both particle-particle and particle wall so that the particles will stick to the bed of the geometry without bouncing it back [34] .
- **Fit particles to region (DEM solids only):** This selection is used with the automatic particle generator to expand the initial particle mesh to extent the region [35].



Figure 23: Fit particles MFix

- **Radiation Temperature:** The radiation temperature has a default value of 293K, and this is applied when the particles are just existing the nozzle and are entering into the rectangular box [36].



Figure 24: Radiation Temperature

CHAPTER 3: POST PROCESSING

The equivalent spherical particles are moving down due to gravity at the initial speed of 4mm/s into the box as shown in figure 25.

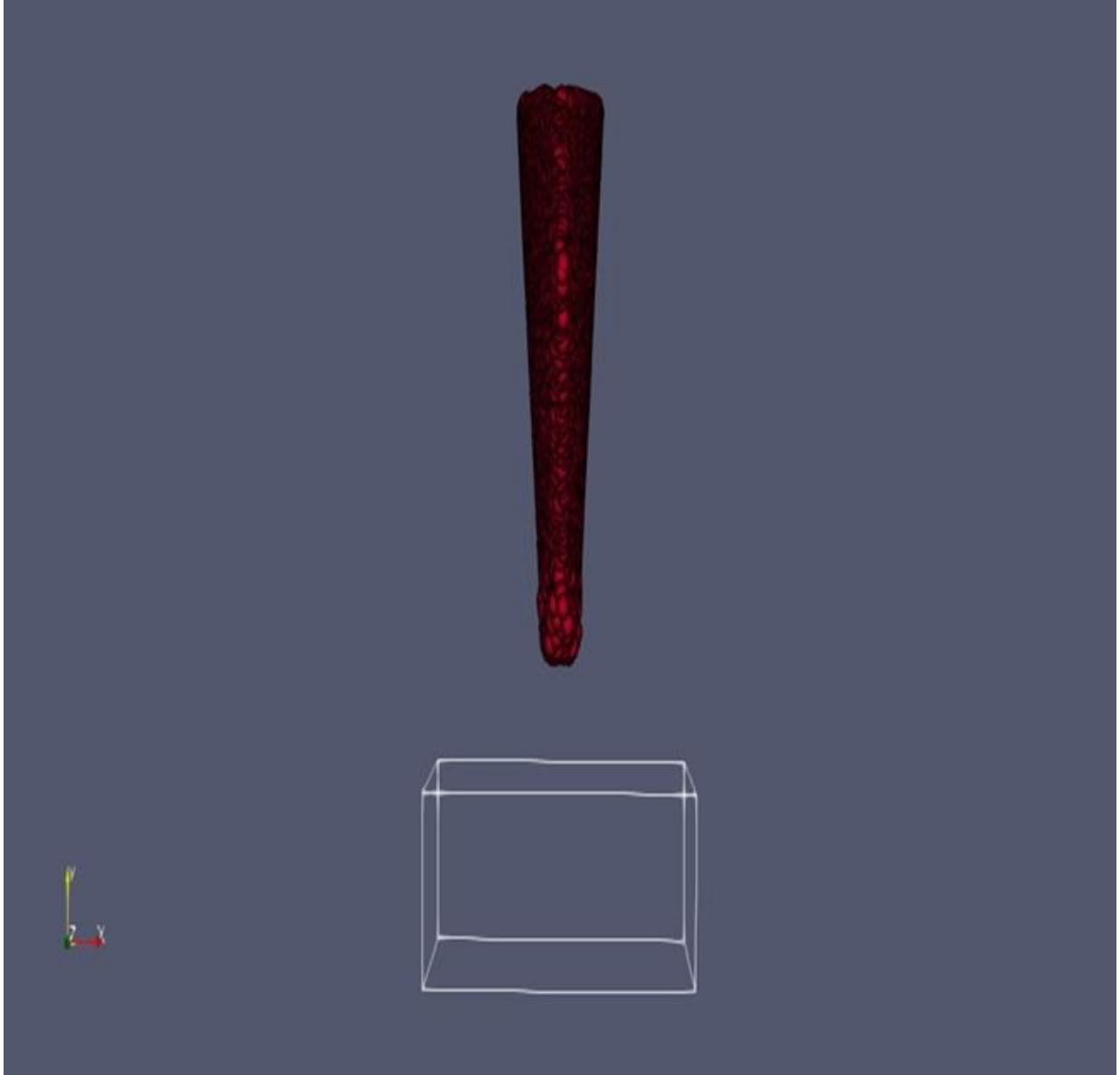


Figure 25: ESP Movement through Nozzle

It has been observed that the temperature distribution over the entire region start changing with respect to time is shown in figure 26, 27 ,28,29,30 and 31 at various time intervals 0.05,0.08,0.12 and 0.14,0.16 and 0.27,0.34 and 0.4s respectively. As the particles start

entering into the rectangular box from stationary source of particles, the temperature of the box start changing gradually decreases in such a manner that as particles strike the bottom of the box it start cooling as the box is assumed to be placed in atmosphere so radiation temperature boundary condition is applied at that place. At 0.05s particles are just entering into the rectangular box and figure shows that at that interval hot particles temperature start changing.

As the particles start touching the bottom of the box, it starts cooling and the figure shown at interval 0.34s indicates the effect of cooling on the deposited layer.

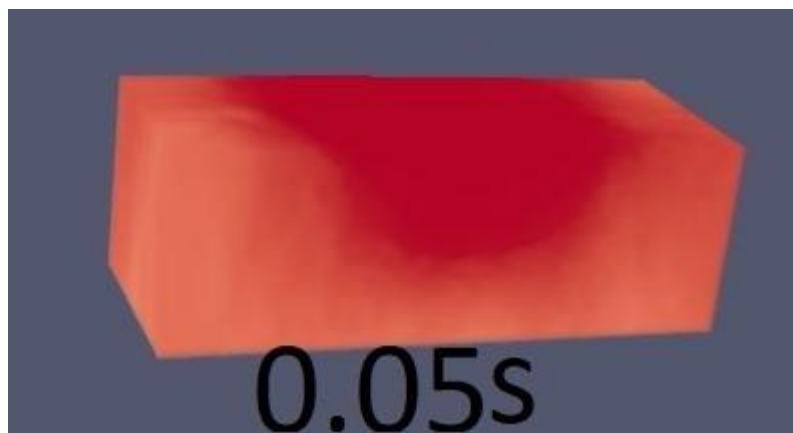


Figure 26: Temperature Distribution at 0.05s

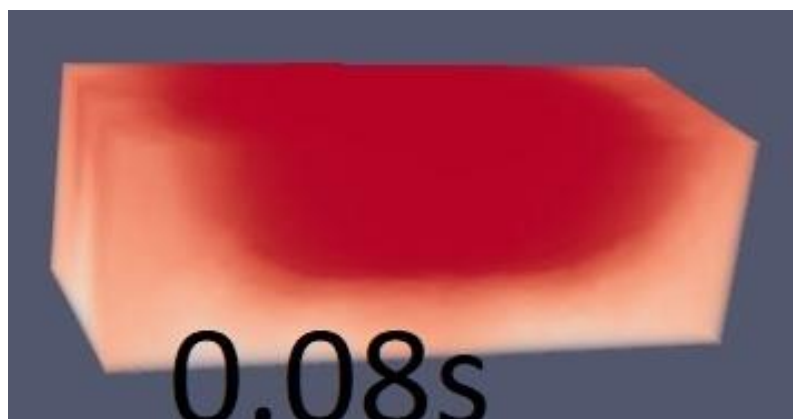


Figure 27: Temperature Distribution at 0.08s

As the particles start touching the bottom of the box, it starts cooling and the figure shown at interval 0.34s indicates the effect of cooling on the deposited layer.

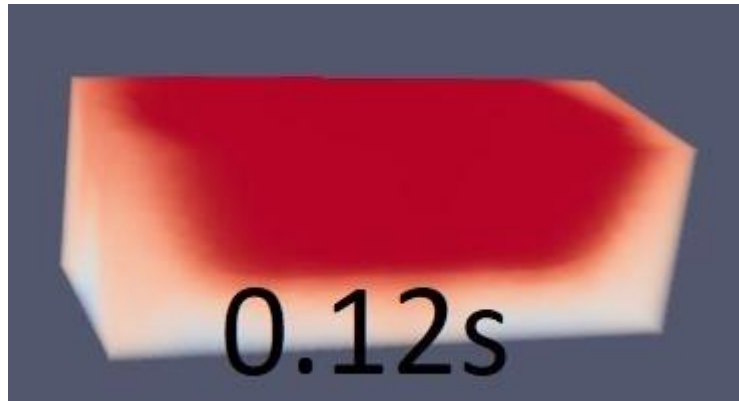


Figure 28 (a): Temperature Distribution at 0.12s

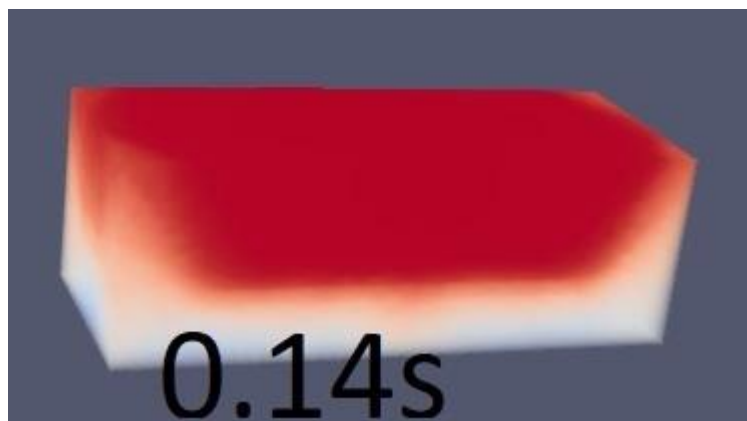


Figure 28 (b): Temperature Distribution at 0.14s

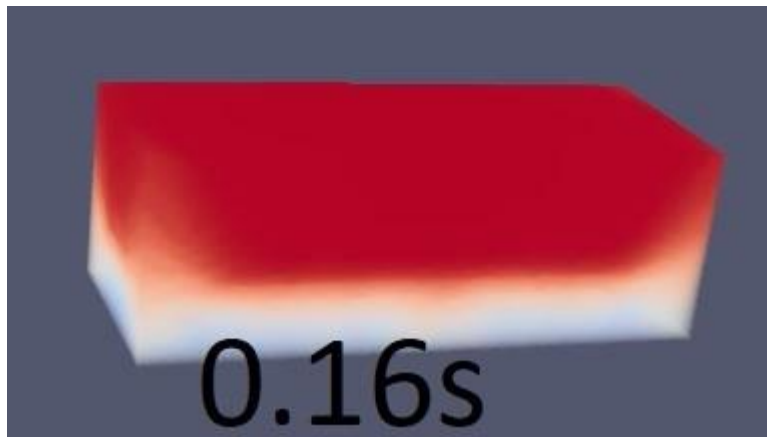


Figure 29 (a): Temperature Distribution at 0.16s

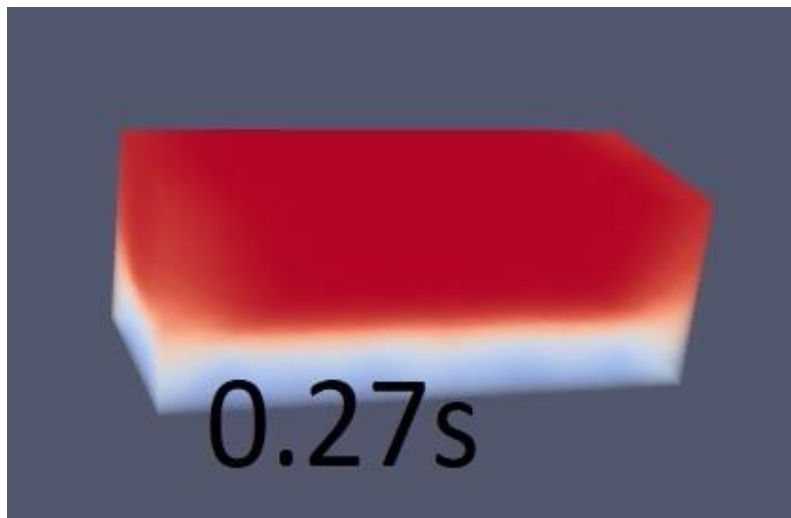


Figure 29 (b): Temperature Distribution at 0.27s

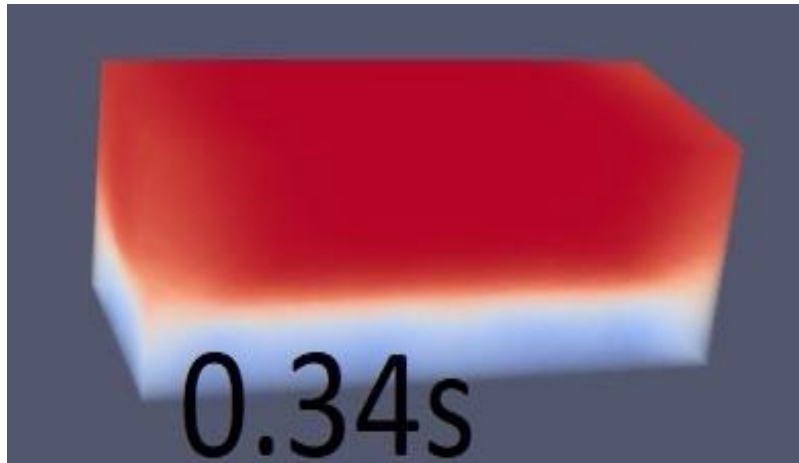


Figure 30 Temperature Distribution at 0.34s

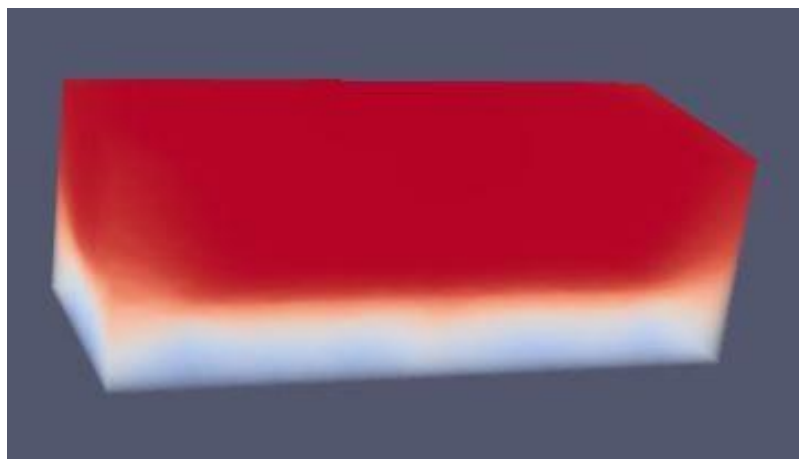


Figure 31 Temperature Distribution at 0.4s

Also in case of 1000W the effect of temperature on the surface with respect to time is as shown in figure 32 and 33 with variation of temperature with respect to time.

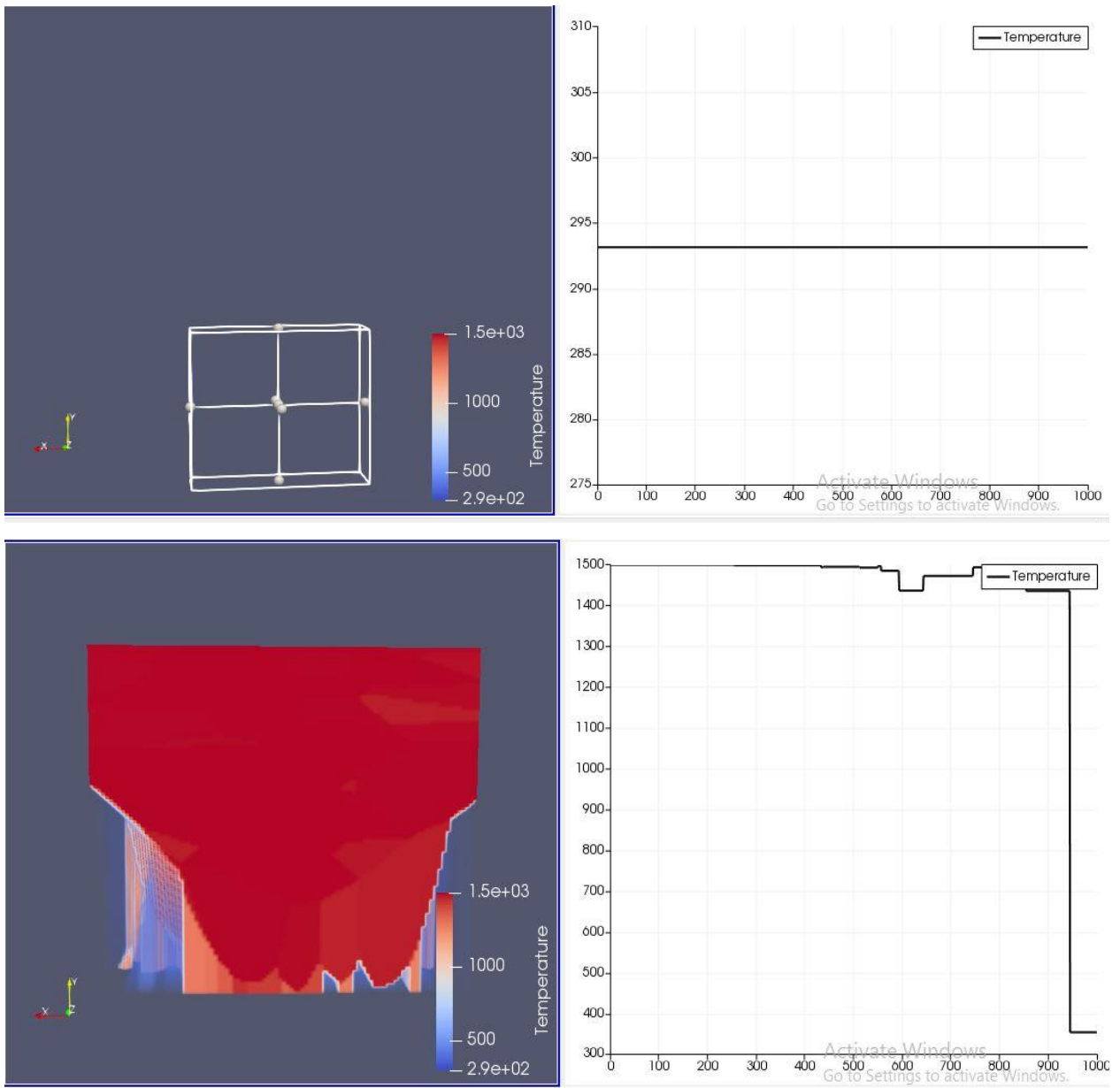


Figure 32(a): Temperature distribution at 0, 0.1s

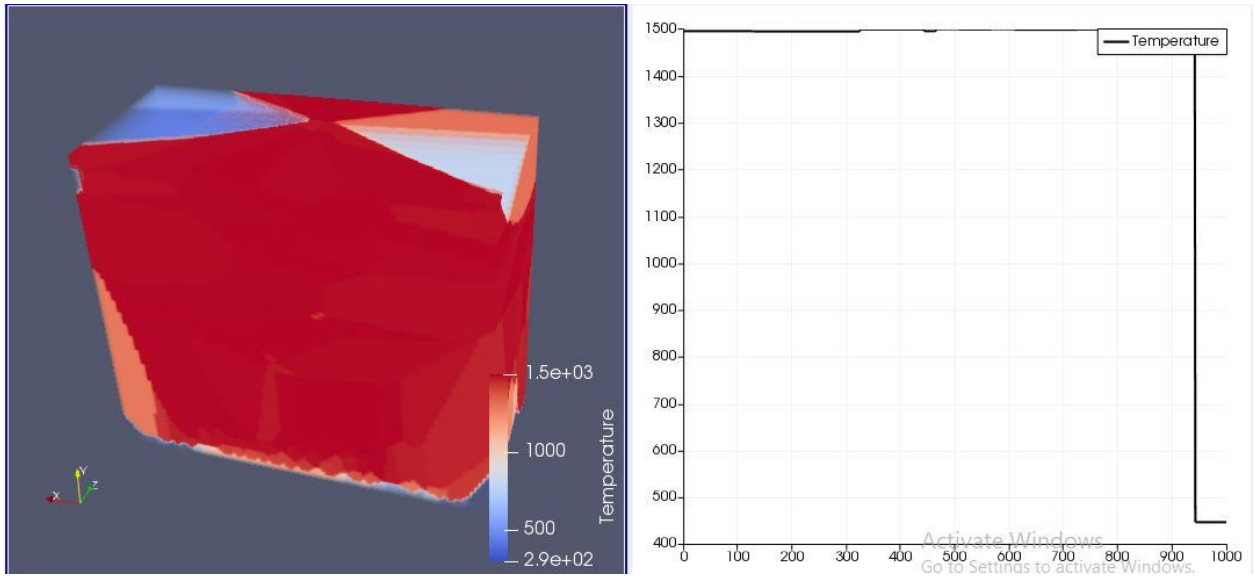


Figure 32 (b): Temperature Distribution at 0.2s

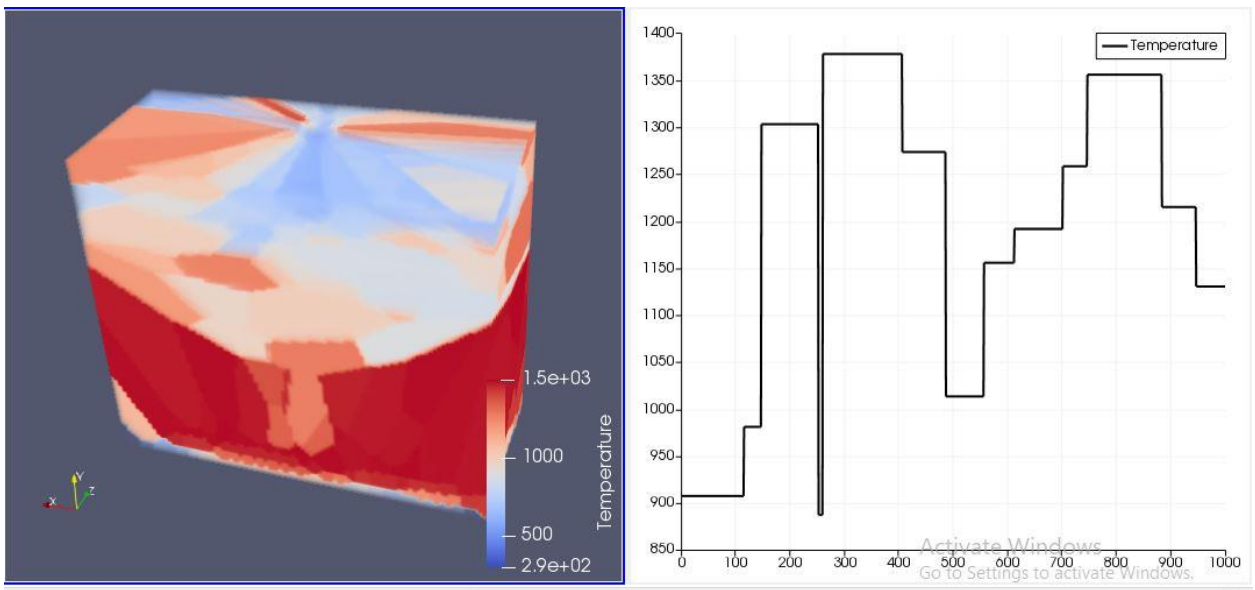


Figure 33(a) : Temperature Distribution at 0.28s

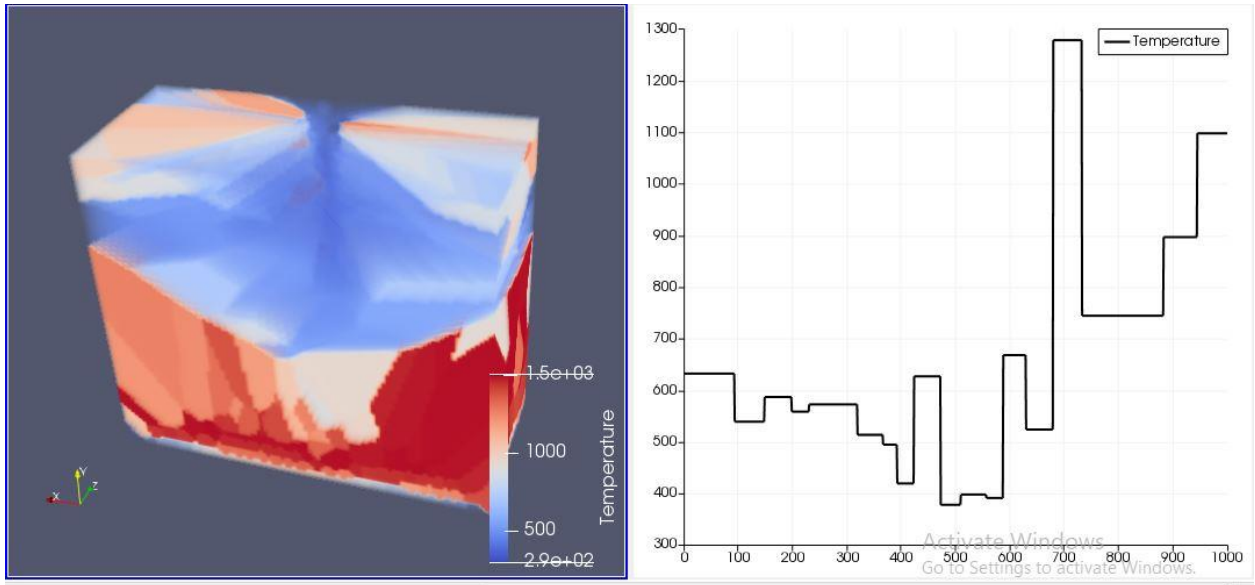


Figure 33(b): Temperature Distribution at 0.3s

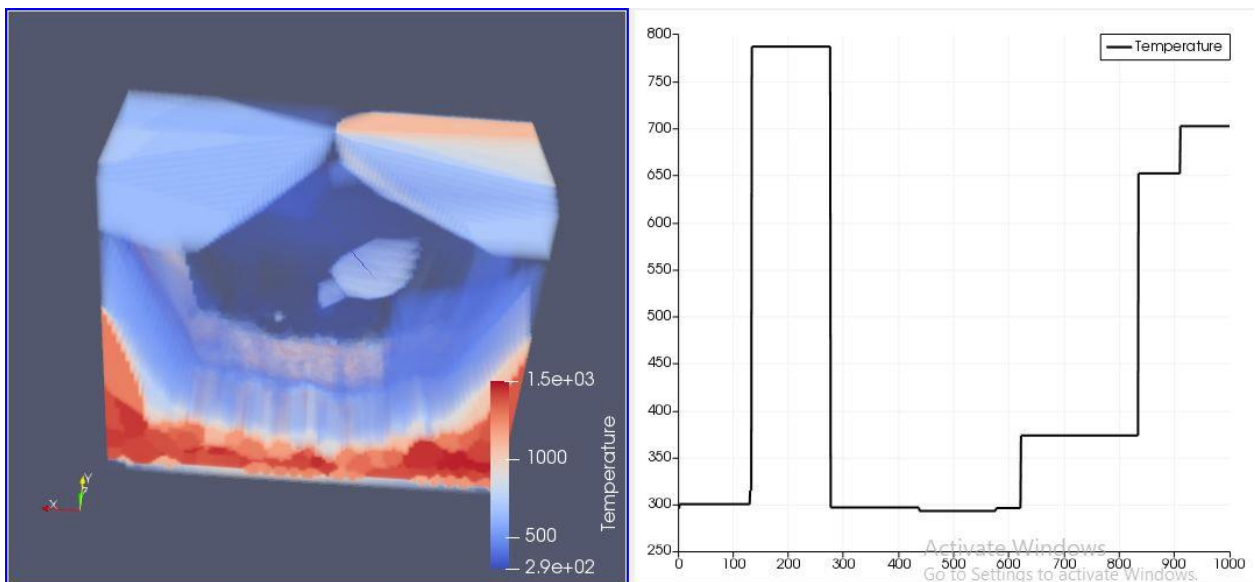


Figure 33(c): Temperature distribution at 0.4s

When particles enter into the rectangular box, its temperature starts changing and equivalent spherical particles solidifies with the change in temperature as shown in figure.

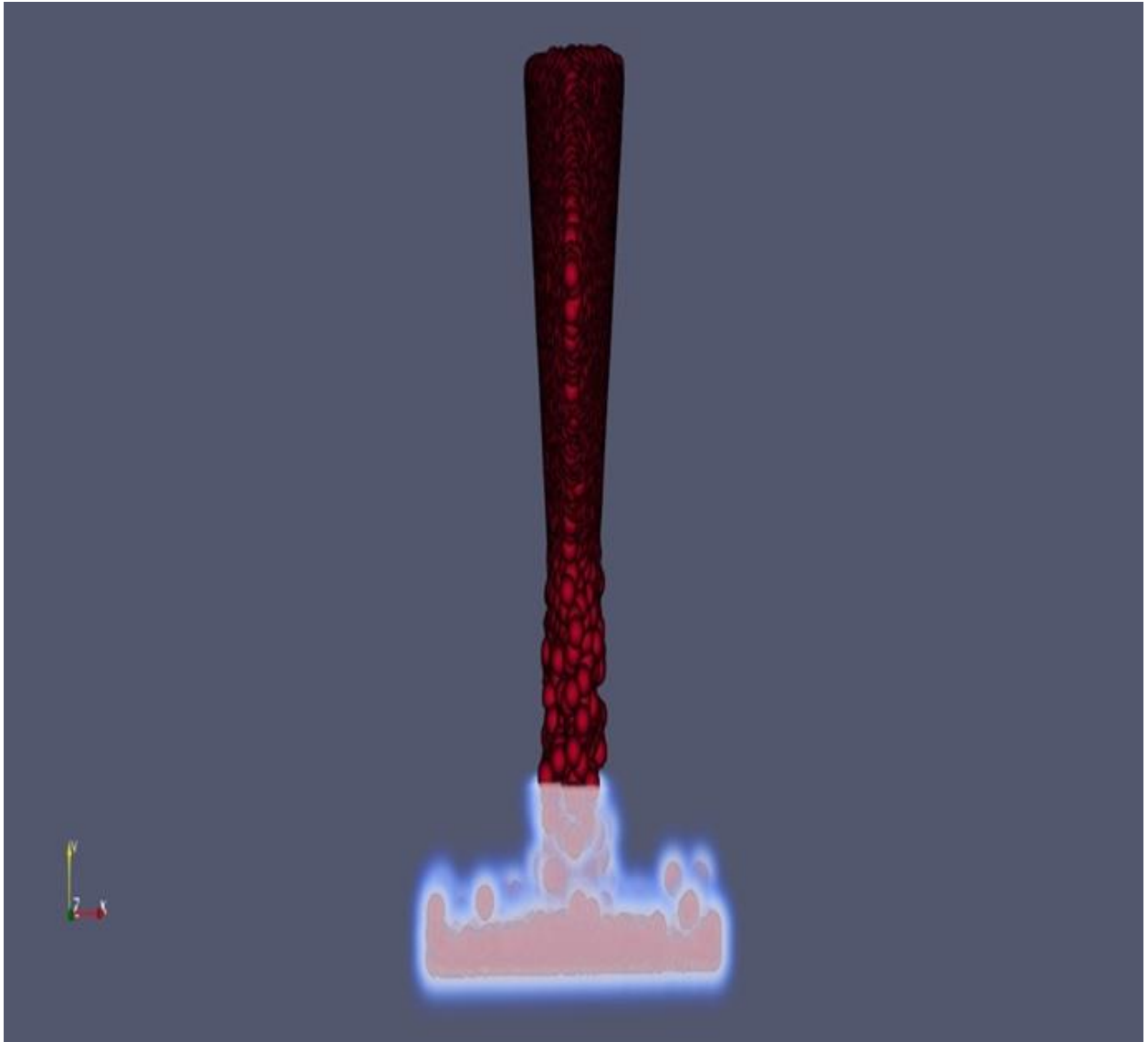


Figure 34: Particle Drop through nozzle exit

In the next figures, it is illustrated that particles after making first layer, another layer of particles are still dropping over the first one to make another layer over first one such that the layer below the second one is continuously cooling and the later one is at highest temperature than the first and it greatly influence the height of the layer build.

The overall sequence of the part build with respect to time is as follows.

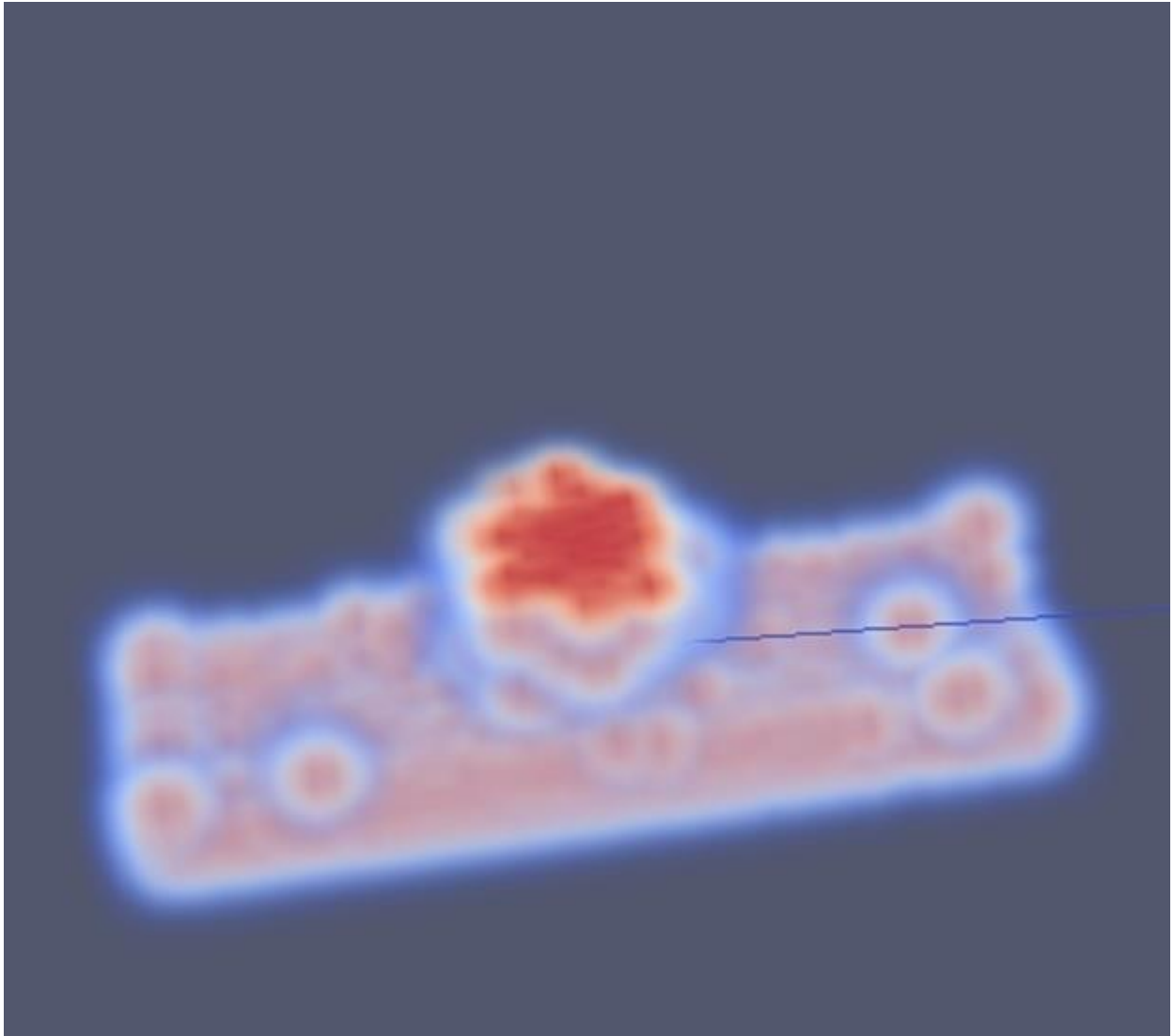


Figure 35: Particle entering the bed

The red spot in figure 35, indicates the laser source where the temperature is changing. The particles start spreading in the geometry until all the particles present in the nozzle dropped into the box to achieve the layer deposition of the particles.

At 0.13s , It has been observed that the deposited layer is much thicker and denser than the figure before.

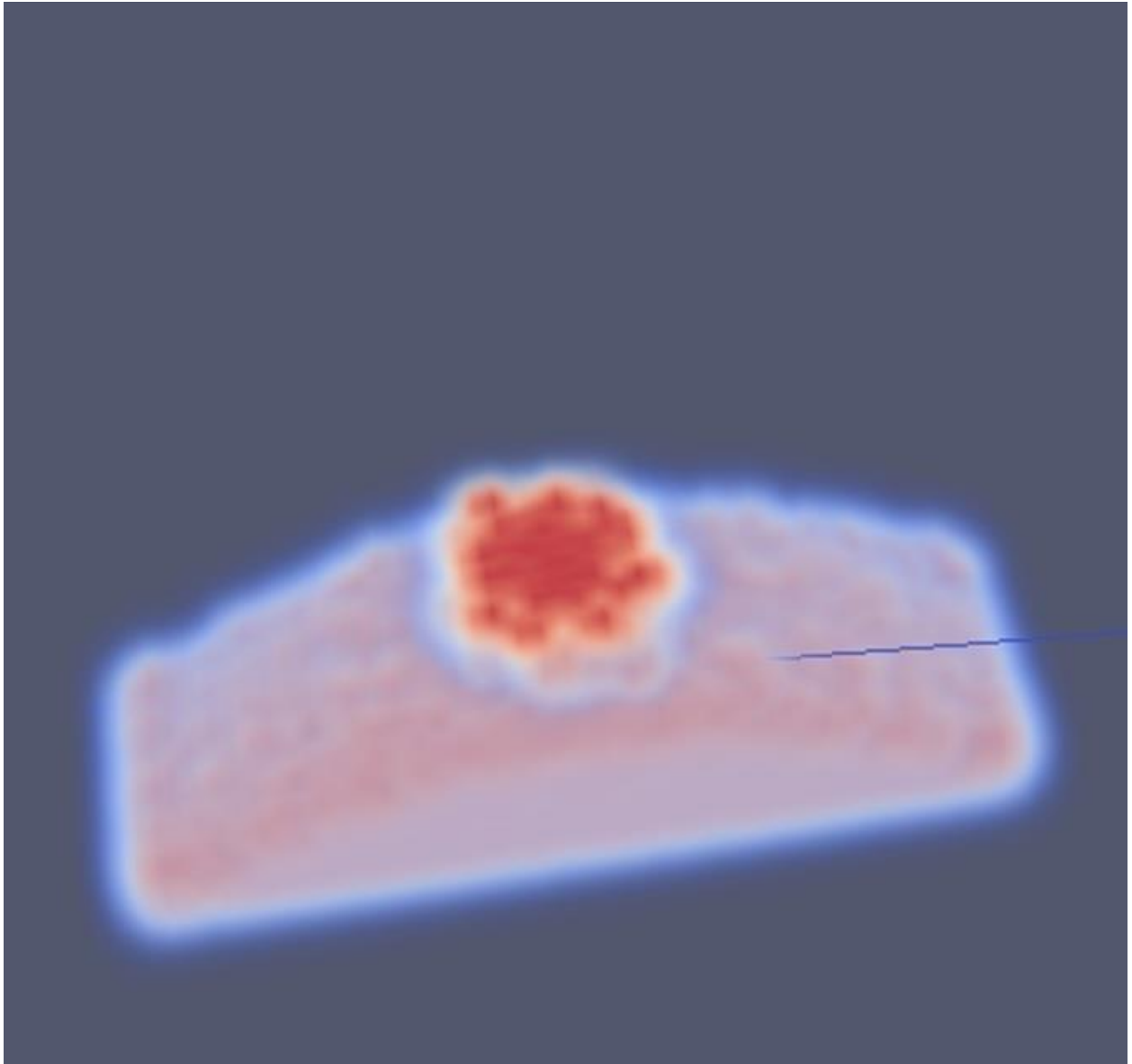


Figure 36: Layer Formation

Figure 37 show the layers formed when all the particles are deposited layer by layer and the layer touching the bottom of the box will cool first and the layer after it will cool after depositing that layer and the effect of it is shown below.

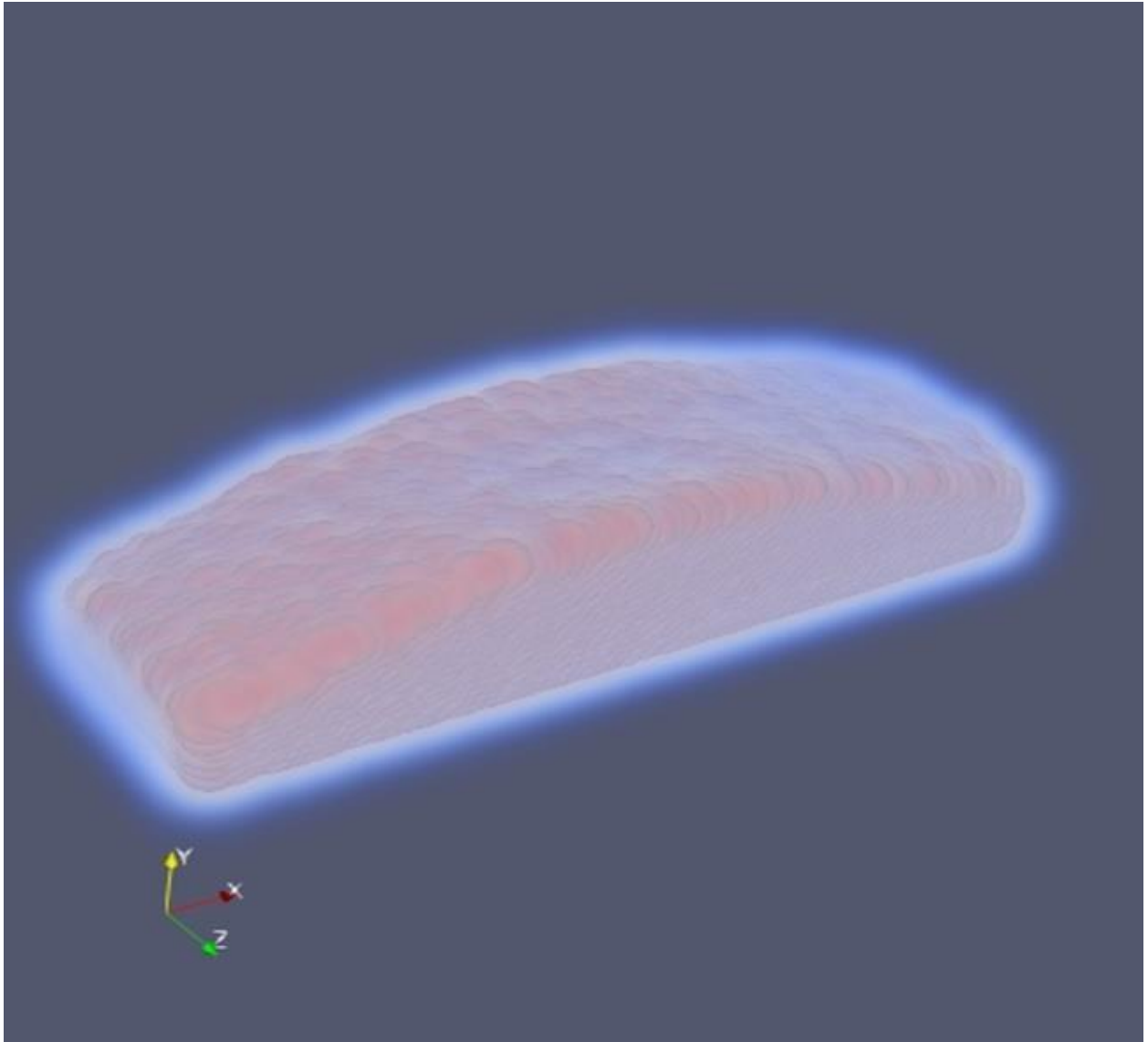


Figure 37: Layer Formation

It has been observed that the layer height obtained at different mass flow rates and powers by altering the values of mass flow rates and laser powers, the following are the graphs obtained for equivalent spherical particles are as follows:

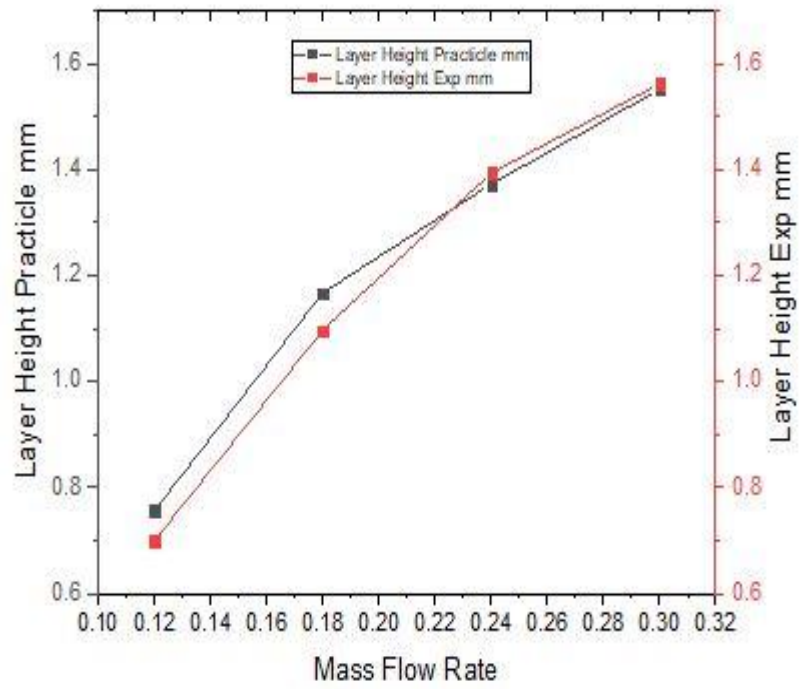


Figure 38: Mass flow rate vs layer height of small shavings at 800W

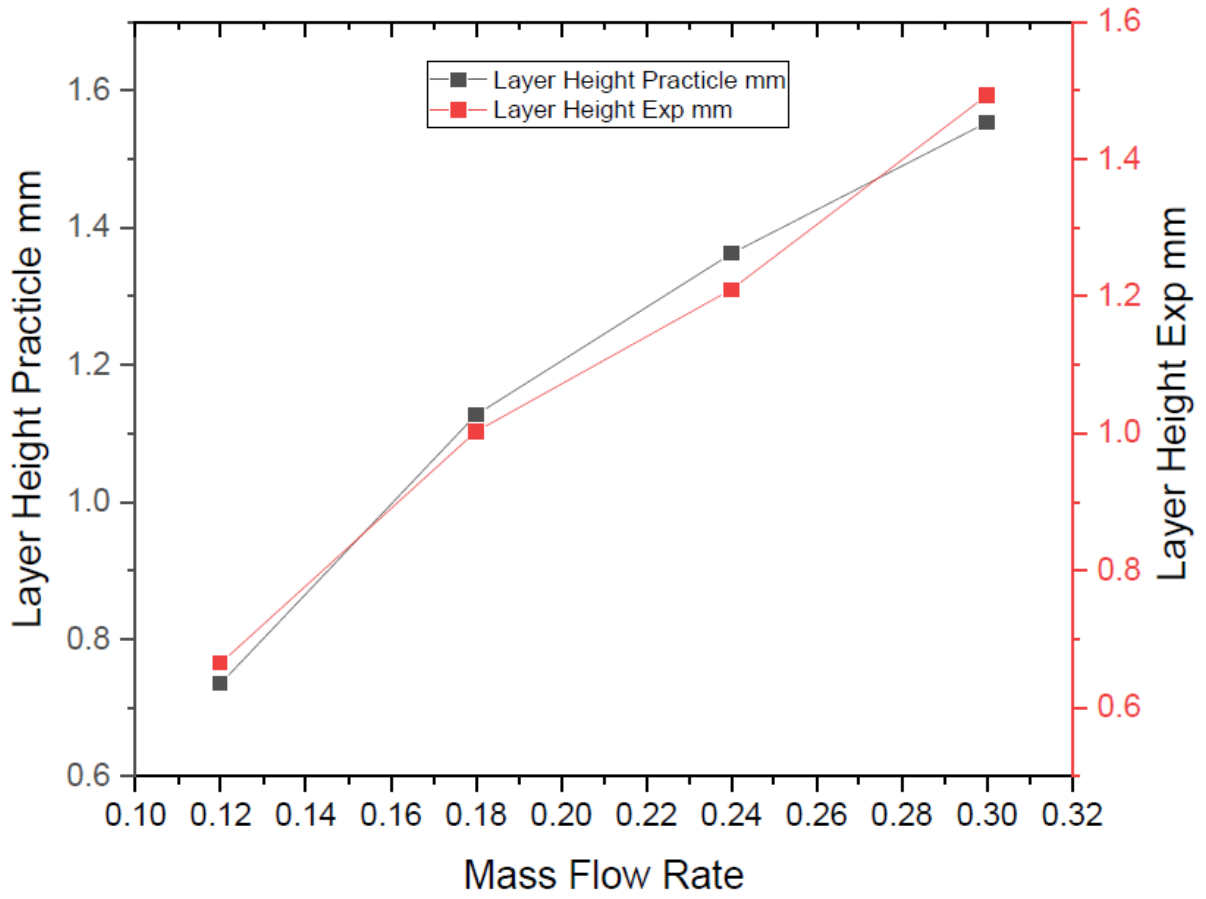


Figure 39: Mass Flow rate vs layer height at 1000W

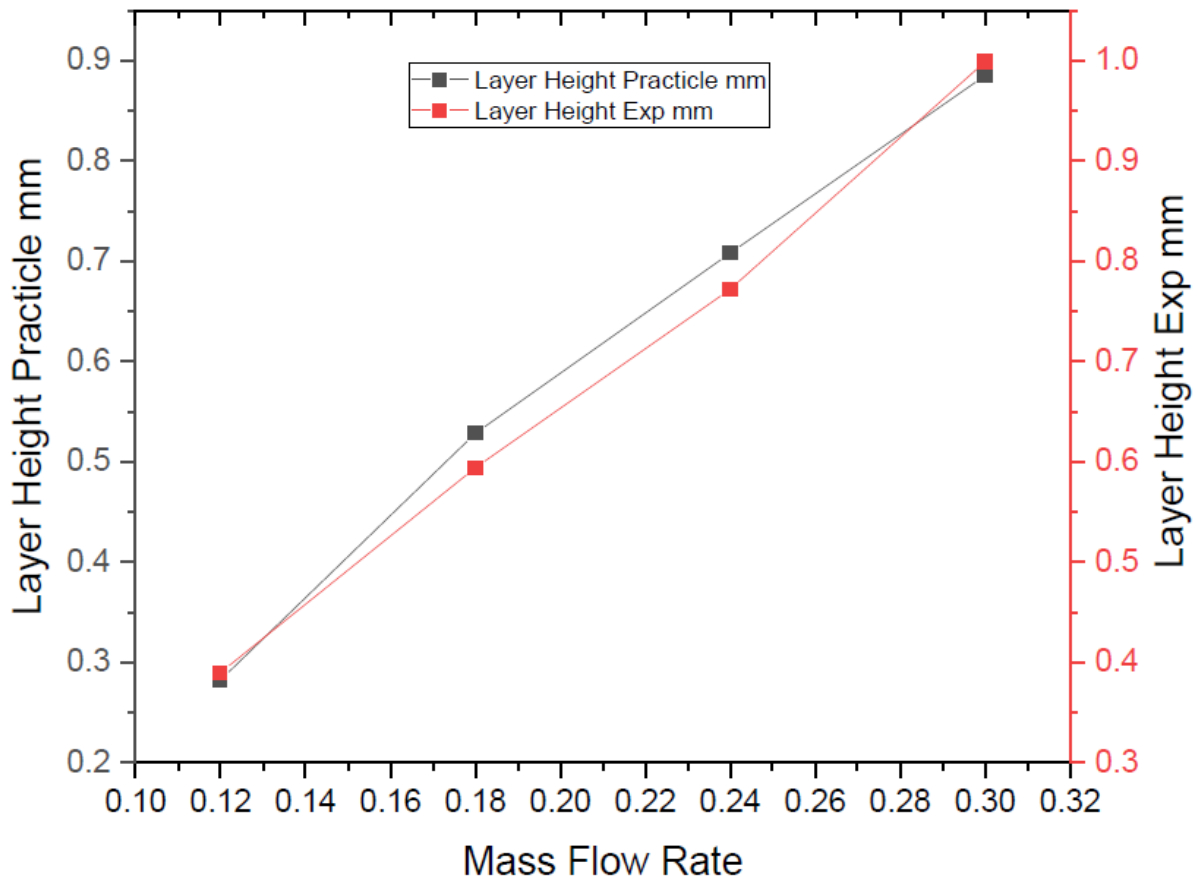


Figure 40: Mass flow rate vs Layer height of large shavings at 800W

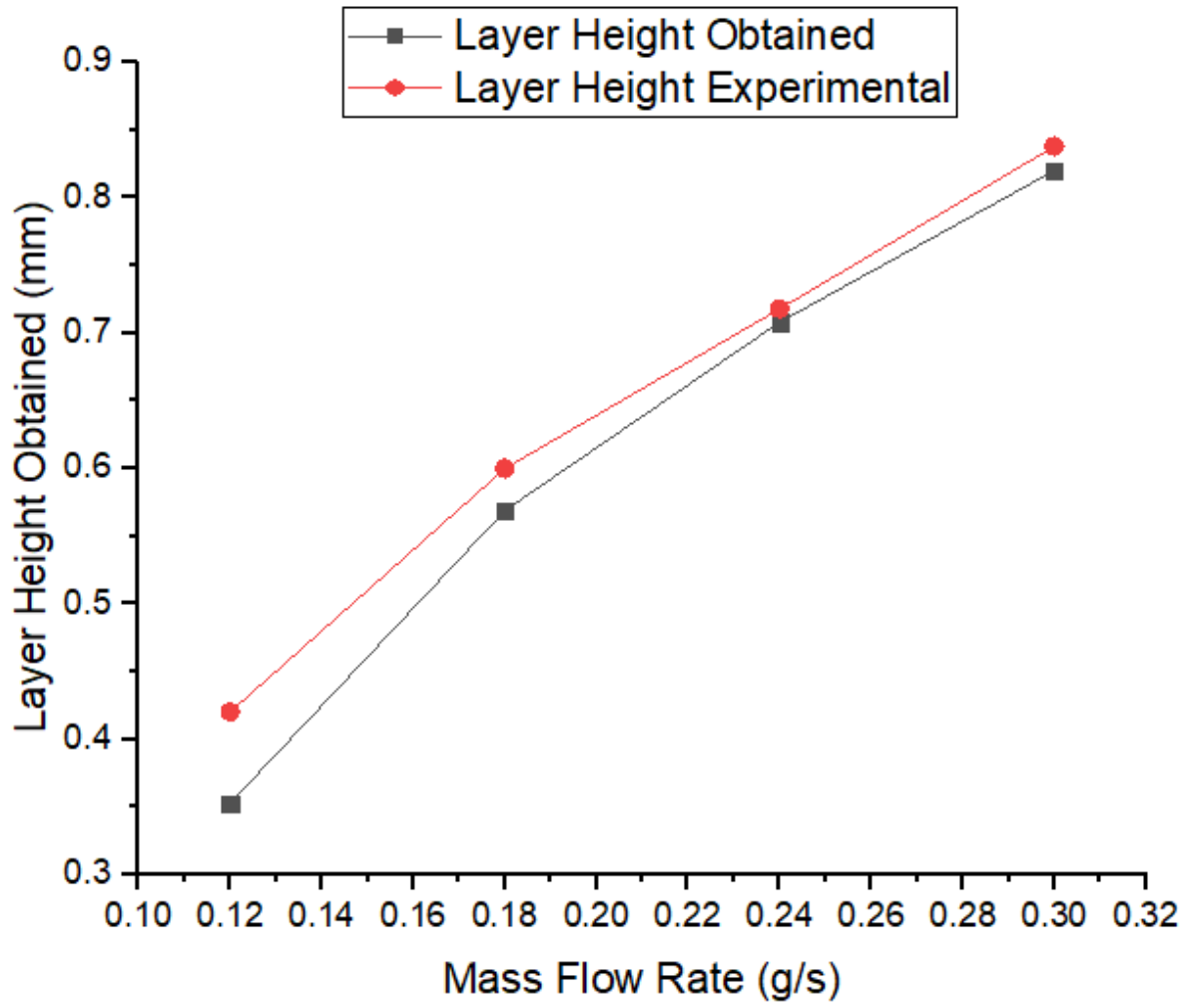


Figure 41: Mass flow rate vs layer height of large shavings at 1000W

CHAPTER 4: RESULTS AND DISCUSSIONS

A Discrete Element Method was conducted to determine the effect of mass flow rate and laser power on the solid region height at the melt pool solidification boundary. It has been observed that the results are in good agreement with the experimental one when the particles are small. As the laser power increases from 800W to 1000W, layer height also increases to some extent showing optimization in the results, but after that increase in laser power will cause reduction in laser height. As the laser power increases temperature increases and high temperature causes the liquid viscosity to decrease, accordingly material can spread out [40]. Also if the morphology of particle changes from SS to LS, a change in layer deposition has been observed. As particle size increases the temperature distribution changes, LS will absorb more energy and it would affect melt pool as more energy would be required to melt the bigger particles and overall deposited height would decrease. Layer height decreased as the particle type changed from SS to LS. It is found that particle morphology is an important parameter while studying powder stream and it affects the whole process. When a particle deviates from its spherical shape it affects powder stream in sense of temperature distribution, particle concentration, and energy attenuation. As particle size increases or decreases from spherical shape, powder concentration and temperature distribution decreases, as bigger and irregular particles will absorb more temperature and concentration will also decrease due to low packing factor.

SUMMARY

A Discrete Element Method using LE approach has been used to evaluate layer height. This model is validated using mass flow rate and laser power to measure the layer height. A Multiphase software is used to measure the layer height by taking the properties obtained from experimental work of material 316L steel. Results indicated that powder feed rate and powder morphology effected the layer height significantly. It was observed from perturbation plot that laser power effected layer height positively.

Conclusion and Future Suggestions

In this thesis, we have focused on the investigation of the effect of processing variables on the geometric features. We have investigated the effect of powder morphology in sub process of DLD. Powder stream is the focus of study and different parameters that can affect the clad height.

DEM Method is used here using LE approach to find a relationship between layer height and major energy and material processing parameters. Where material properties and processing parameters are taken from experimental data. Laser Power, Mass flow rate, particle size and morphology have been considered as active variables. A validation from an existing experimental work has been done. It is found that particle morphology is an important parameter while studying powder stream and it affects the whole process. When a particle deviates from its spherical shape it affects powder stream in sense of temperature distribution, particle concentration, and energy attenuation. As particle size increases or deviates from spherical shape, powder concentration and temperature distribution decreases, as bigger and irregular particles will absorb more temperature and concentration will also decrease due to low packing factor. Discrete Element method is the best method to compute laser deposition process, besides EE approach one should focus on DEM method for more appropriate results. Also, this work can be extended furtherly by moving the nozzle above the substrate. Different mechanical properties can be achieved using this method.

REFERENCES

- [1] Choi. J, 2002, “Process and Properties Control in Laser Aided Direct Metal/Materials Deposition Process” Proceedings of IMECE, New Orleans LA November 17-22
- [2] T.B. Anderson, R. Jackson,1967, A fluid mechanical description of fluidized beds.
- [3] M. Ishii,1975, Thermo-Fluid Dynamic Theory of Two-Phase Flow, Eyrolles, Paris .
- [4] D. Gidaspow,1994, Multiphase Flow and Fluidization: Continuum and Kinetic Theory
- [5] C.K.K. Lun,1984, Kinetic theories for granular flow inelastic particles in Couette flow
- [6] D. Gidaspow,1983 ,London Fluidization in two-dimensional beds with a jet ,Industrial and Engineering Chemistry Fundamentals 22 (2) (1983) 193–201.
- [7] Y.P. Tsuo, 1990, Computation of flow patterns in circulating fluidized beds,Paris.
- [8] M.A. van der Hoef, 2006, Multiscale modeling of gas-fluidized beds,Paris
- [9] G.V. Middleton, 1984, Mechanics of Sediment Movement 2nd ed Society of Economic
- [10] A. Prosperetti, 2007, Computational Methods for Multiphase Flow, 1st ed,
- [11] C.T. Crowe, 2011, Multiphase Flows with Droplets and Particles, Boca Raton.
- [12] Subramaniam, 2013, Lagrangian–Eulerian methods for multiphase flows. Progress in Energy and Combustion Science, pp 215-245.
- [13] P. Gondret, 2002, Bouncing motion of spherical particles in fluids, Phys Fluids 14 643.
- [14] https://www.nabertherm.com/produkte/additivefertigung/en?gclid=EAIaIQobChMIpPXgn5Lr6AIV2ed3Ch1oPwpIEAAYASAAEgI_hvD_BwE
- [15] Thorn, 1982, The Interaction of Process Variables-Their Influence on Weld Dimensions in GMA Welds on Steel Plates, Metal Construction Vol 14.
- [16] Esser, W.G, 1981, Heat Transfer and Penetration Mechanisms with GMA and Plasma GMA Welding, Welding Journal Vol 60.
- [17] Lagutkin, 2004, Atomization process for metal powder. Materials Science and Engineering: A, 383(1) pp.1-6.
- [18] Pinkerton, 2005, Direct additive laser manufacturing using gas-and water-atomised H13 tool steel powders. The International Journal of Advanced Manufacturing Technology, 25(5-6) pp.471-479.
- [19] Z Fan and F Liou,2012, Numerical Modeling of the Additive Manufacturing (AM) Processes of Tita-nium Alloy University Campus STeP Ri, Slavka Krautzeka 83/A 51000 Rijeka, Croatia InTech Europe.
- [20] Aldrich, R., 2000, Laser fundamentals

- [21] K. and Ye, 2006, Laser shock peening: performance and process simulation, Woodhead Publishing.
- [22] Konert, 1997, Comparison of laser grain size analysis with pipette and sieve analysis: a solution for the underestimation of the clay fraction. *Sedimentology*, 44(3) pp.523-535.
- [23] Eshel, 2004, Critical evaluation of the use of laser diffraction for particle-size distribution analysis. *Soil Science Society of America Journal*, 68(3) pp.736-743.
- [24] Huang, 2006, Three-dimensional analytical model on laser-powder interaction during laser cladding. *Journal of Laser Applications*, 18(1) pp.42-46.
- [25] Liu Q & Brandt M, (2017), Repair and manufacturing of military aircraft components by additive manufacturing technology. In 17th Australian International Aerospace Congress: AIAC 2017 (p. 363). Engineers Australia, Royal Aeronautical Society.
- [26] Ahn, 2011, Applications of laser assisted metal rapid tooling process to manufacture of molding & forming tools—state of the art, *International Journal of Precision Engineering and Manufacturing*.
- [27] Toyserkani, 2004. Laser cladding, CRC press.
- [28] Toyserkani E and Khajepour. , 2005, “Laser Cladding” CRC Press, LLC, Boca Raton, Florida pages 280.
- [29] Taberner, 2014, “Modeling of the geometry built-up by coaxial laser material deposition process” *Int J of Advanced Manuf Technology*, vol.70
- [30] Hou, 2017, Improving interfacial, mechanical and tribological properties of alumina coatings on Al alloy by plasma arc heat-treatment of substrate, *Appl Surf Sci*.
- [31] Selcuk, 2013, Joining processes for powder metallurgy parts, In *Advances in Powder Metallurgy* (pp. 380-398) Woodhead Publishing.
- [32] R. Garg, J, 2012, Documentation of open-source MFI-X-DEM software for gas–solids flows, Computer Science and Mathematics Division, Oak Ridge National Laboratory Oak Ridge TN.
- [33] Mahmood and Pinkerton, 2013, Direct laser deposition with different types of 316L steel particle: a comparative study of final part properties. *Proceedings of the Institution of Mechanical Engineers, Part B: Journal of Engineering Manufacture*.
- [34] R. Garg, 2012, Documentation of open-source MFI-X-DEM software for gas–solids flows, Computer Science and Mathematics Division Oak Ridge National Laboratory.
- [35] R. Garg, 2012, Open-source MFI-X-DEM software for gas–solids flows: part I — verification studies, *Powder Technol*.

- [36] R. Garg,2012, Open-source MFIX-DEM software for gas–solids flows: part II — validation studies, Powder Technol. 220 138–150
- [37] Peter S,2020, Simulation of melt pool behaviour during additive manufacturing, Underlying physics and progress
- [38] Graf, 2013, Design of experiments for laser metal deposition in maintenance repair and overhaul applications, Procedia CIRP.
- [39] Mazumder, 2002,Fabrication of biomedical implants using direct metal deposition, U.S. Patent Application 09/916 976.
- [40] Liu, S. and Kovacevic, 2014, Statistical analysis and optimization of processing parameters in high-power direct diode laser cladding. The International Journal of Advanced Manufacturing Technology 74(5-8) pp.867-878.

CERTIFICATE OF COMPLETENESS

It is hereby certified that the dissertation submitted by *NS Mursaleen Shahid* , Registration No.00000204954, Titled: “*Modeling of the effect of non-spherical particles of various sizes using Direct Laser Deposition (DLD)*” has been checked/reviewed and its contents are complete in all respects.



Signature of Supervisor
(Dr. Khalid Mahmood)